Undergraduate Honors Theses   Theses, Dissertations, & Master Projects

4-2014

Studies Directed toward the Synthesis of Asymmetric Loline Alkaloids

Kelsey E. Miller
College of William and Mary

Follow this and additional works at: https://scholarworks.wm.edu/honorstheses

Part of the Organic Chemistry Commons

Studies Directed toward the Synthesis of Asymmetric Loline Alkaloids

A thesis submitted in partial fulfillment of the requirement
for the degree of Bachelor of Science in Chemistry from
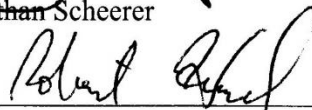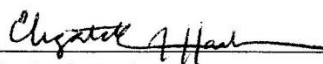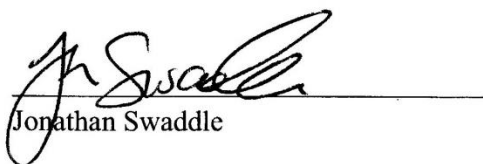The College of William and Mary

by

Kelsey Miller

Accepted for Honors

_____
Jonathan Scheerer

_____
Robert Hinkle

_____
Elizabeth Harbron

_____
Jonathan Swaddle

Williamsburg, VA

April 29, 2014

ABSTRACT PAGE

This thesis discusses the progress toward the synthesis of asymmetric loline alkaloids. Lolines are polycyclic pyrrolizidine alkaloids that contain four contiguous stereocenters and a strained ether bridge. Lolines are present in symbiotic relationships between grass species and fungal endophytes and act as a natural pesticide and feeding deterrent that protects the grass host from insects, yet are believed to possess low toxicity to mammals. Our Scheerer 2nd generation synthesis takes precedent from the 1st generation Scheerer synthesis, but with some key changes. The synthetic route has fewer steps, a different nitrogen protecting group, and usage of stereoselective tethered aminhydroxylation 3rd generation conditions. Other key reactions include Petasis borono-Mannich addition and ring closing metathesis using Hoveyda-Grubbs 2nd generation catalyst.

TABLE OF CONTENTS   Page

DEDICATION

For my parents, Mark and Wynne Miller, and my sister, Courtney, who have always been

wonderful role models in the realm of academia.

LIST OF FIGURES

LIST OF TABLES

LIST OF SCHEMES

8

CHAPTER I

THE HISTORY OF LOLINE ALKALOIDS

Introduction:

      The art of total synthesis involves chemically making a molecule, commonly a natural product, from simple starting materials.[1] The goal is to synthesize the target molecule in the most efficient way with commercially available reagents and starting materials. The first step of designing a synthetic plan is choosing a target molecule. This thesis explains the steps toward synthesizing loline alkaloid.

loline
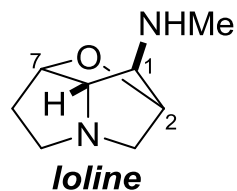
The Alkaloid Family involved in Grass-endophyte Symbioses:

Alkaloid is a general term for any compound containing nitrogen and they can be a secondary metabolite produced by plants, animals, bacteria, or fungi.[3] Secondary metabolites are substances that are not directly involved in the organism's growth, diet, or reproduction.[17] This evolutionary adaptation is hypothesized to serve as an organism's defense mechanism, especially in plants.[18] In the context of this thesis, alkaloids produced by fungi, namely fungal endophytes *Neotyphodium* and *Epichloë*, with a symbiotic relationship with grasses will be discussed. These fungal endophytes produce the alkaloids in exchange for the plant's nutrients and in return the alkaloids provide the host with a defense mechanism.[2] There are four classes of alkaloids that are involved in grass-endophyte symbioses, which consist of lolines, peramine, indole diterpenes, and ergot alkaloids (**Figure 1.1** for examples of derivatives from each alkaloid class).[3]

Figure 1.1: Four classes of alkaloids in grass-endophyte symbioses

ergovaline

peramine

loine

lolitrem B
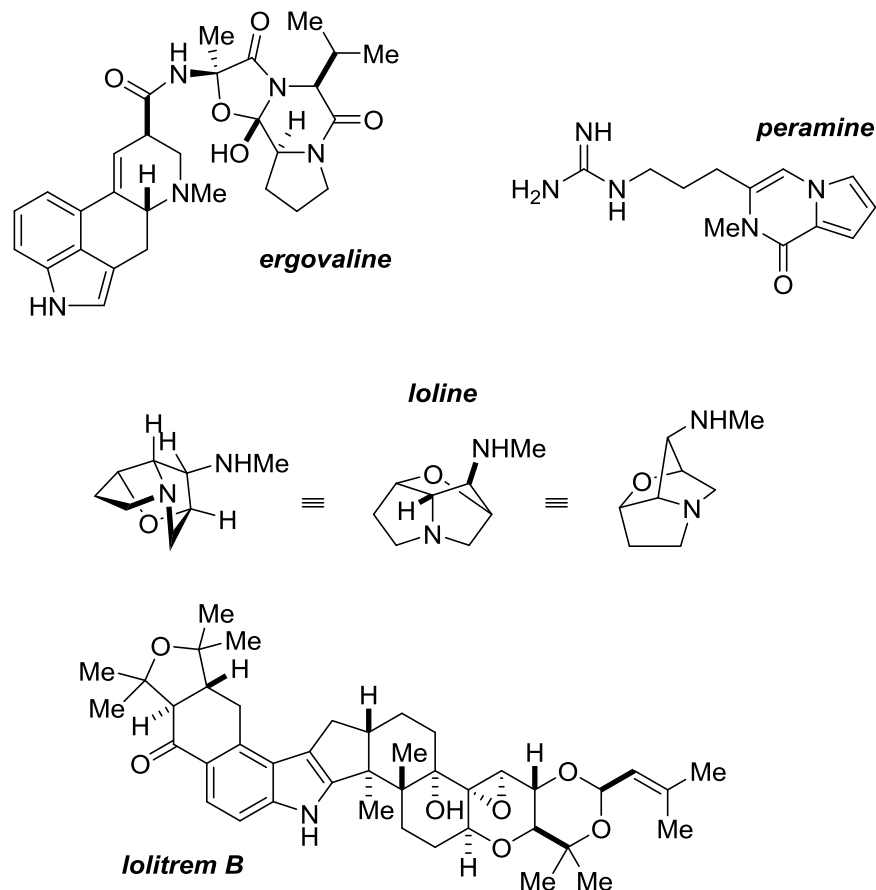
Lolines are saturated pyrrolizidines that are a natural feeding deterrent to insects.[3] There are multiple forms of loline alkaloids, but the most common lolines include *N*-norloline, *N*-acetylloline, *N*-acetyl norloline, and *N*-formylloline (**Figure 1.2** for loline homologues). Peramines are isolated pyrrolopyrazine alkaloids that act as a feeding deterrent to insects, as well. There are no homologues of peramine. Indole diterpene alkaloids have multiple variants with the most common being lolitrems, which cause muscle tremors in vertebrates. Specifically, lolitrem B causes ryegrass stagger disease in animals. Ergot alkaloids include clavines with an ergoline ring system and lysergic acid and its many derivatives.[4] The main ergot found in symbiota is ergovaline, which is responsible for intoxications among vertebrates and even

humans.[3] Indole diterpenes and ergots are considered mainly as vertebrate feeding deterrents, but they may possess anti-invertebrate properties, as well.

Infected grasses are asymptomatic and do not show any external signs of the fungi, even though they systemically infect the host.[4] However, endophytes can be detected by histochemical or serological analysis.[19] Specifically, tissue print-immunoblot (TPIB) and protein A-sandwich ELISA (PAS-ELISA) methods are employed when detecting endophyte-infected fields. Using these detection techniques furthers our understanding about which specific grasses produce endophytes and what endophytes exist.

The grass-endophyte association is complex, but the symbiotic relationship can be mutualistic in that the fungi depend on the grass for nutrients and in return the alkaloids produced by the fungi enhance host fitness factors.[4] For example, there may be increased plant growth, fecundity, and a higher tolerance to drought stress. In addition, alkaloids offer the grass a defense mechanism by giving the plant anti-insect and/or anti-vertebrate protection. Damaging the grass tissue may result in an increased production of alkaloids.[2] In an experiment by Craven and co-workers meadow fescue with *Neotyphodium siegelii* producing multiple forms of loline increased in plant dry weight in eleven days after clipping.[20] These results of endophyte response to environmental stresses suggest signaling between the host and symbiont. The mechanism behind this communication is not well understood, but the relation between the plant and the fungal species poses many research avenues that have yet to be explored.

The alkaloids are localized and produced by the endophyte within the plant depending on the plant's life cycle. *Epichloë* endophytes have evolutionary adapted to mutualistic relationships with grasses because they have an extremely regimented intercellular growth within the host plant.[5] Endophyte growth is well-coordinated with the grass's growth since it

synchronizes its maturation rate according to plant tissue differentiation. The hyphae enter the embryo before seed maturation and after seed germination, but hyphae never enter the roots or anthers. Additionally, the hyphae do not break the host cell walls nor are there obtrusive feeding structures. It is unknown whether the plant's defense mechanism is suppressed or if the endophyte is truly that conspicuous. Localization of the alkaloid is an important factor when observing what plant tissues herbivores consume.[4] Loline alkaloids tend to be located in spikelet, flower stem, rachis, and leaf blades. Ergots and peramines are usually located in the pseudostem, while indole diterpenes are most concentrated in the leaf sheath. Generally, the highest concentration of toxins lies in the leaf sheath and pseudostem and the least amount in the leaf blades. For example, during high grazing pressures herbivores tend to eat the lower portions of fescue and ryegrass plants more than usual and this is where the toxins are more concentrated; thus, toxicosis rates increase. In addition, in stressful, warm season environments the infectivity levels of the grasses increase, so once again there is a positive correlation of fescue toxicosis in grazing cattle. Other vertebrates are affected too. Multiple studies have shown a lower capture rate of small mammals in endophyte-infected tall fescue field plots compared to non-infected fields. Specifically, one study found reduced vole (*Microtus ochrogaster*) reproduction in infected plots.[5] In one experiment, Canada Geese (*Branta canadensis)* that grazed in endophyte-infected grass lost weight compared to Canada Geese that gained weight in non-infected grass.[6] Another recent study in 2013 showed that peramine and lolitrem B travel up through the food chain after aphid predators ingested aphids feeding on endophyte-infected grass.[7] Additionally, one study showed that ergovaline bioaccumulates in saphenous veins with repeated exposure *in vitro*.[21] This bioaccumulation may explain the toxicities seen in herbivores grazing in endophyte-infected grass. Grass-endophyte symbioses are usually beneficial to the plant, but

may pose consequences to the food chain. More studies must be performed to observe the effects of alkaloids on higher trophic levels, especially since lolines and peramines are the only alkaloids with inconclusive results about consequences to vertebrates. Furthermore, more work must be performed to determine if bioaccumulation of these four classes of alkaloids occurs in grazing animals. The grass-endophyte relationship is complex because multiple alkaloids can exist in one host plant, so pinpointing what exact alkaloid is causing sicknesses in herbivores is difficult.

Loline alkaloids:

After widespread outbreaks of livestock toxicosis in the 1800s researchers began investigating a chemical compound causing these sicknesses.[2] Researchers linked the ryegrass *Lolium temulentum* to the epidemic and through multiple studies at different times, eventually identified that a network between a symbiotic fungus and a new group of secondary metabolites existed. In 1892 Hofmeister became the first to isolate a loline alkaloid from *Lolium temulentum* to which he gave the elemental formula $C_7H_{12}N_2O$ and deemed the compound temuline, which is now known as norloline. Although many structures were proposed after 1892, it was not until almost a century later in 1966 that the correct structure was introduced. Yunusov and Akramov's structure composed of a tricyclic system with an *endo-N*-methyl-1-aminopyrrolizidine core with a C2–O–C7 bridge. In 1969 Aasen and Culvenor confirmed Yunusov and Akramov's proposed structure with IR and proton NMR spectroscopic analyses.

Lolines are polycyclic pyrrolizidines that contain four stereogenic centers. These stereogenic centers consist of an *exo*cyclic amine at C1 and an ether bridge connecting C2 and C7. The amine at C1 can be found with acyl or alkyl substitutions. Representatives of loline are presented in three views (**Figure 1.2**). There are many more derivatives than only six.

Figure 1.2: Different representatives of loline alkaloids

R^1	R^2		
Me	H	**1**	loline
Me	Me	**2**	methylloline
H	H	**3**	norloline (temuline)
Me	Ac	**4**	acetylloline (lolinine)
Me	CHO	**5**	formylloline
H	Ac	**6**	acetylnorloline
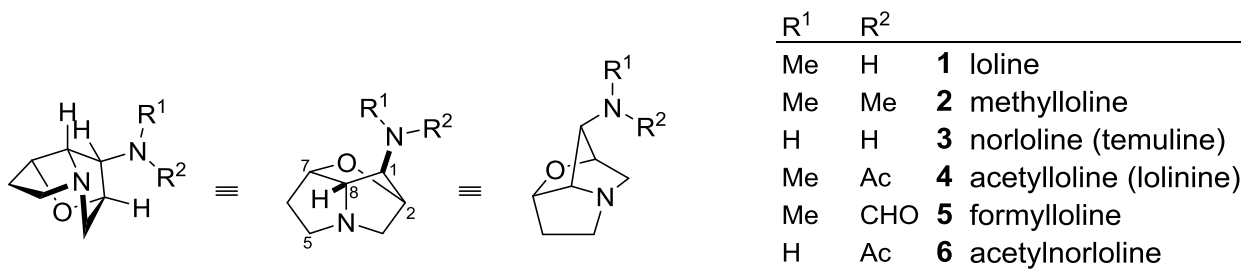
Originally, loline alkaloids received negative attention due to their association to livestock toxicity, but researchers eventually realized that ergot alkaloids were the ones causing harm to mammals. Actually, loline alkaloids act as a natural pesticide and feeding deterrent that protect the grass from insects, yet are believed to possess low toxicity to mammals. Studies suggest that the acyl and alkyl substitutions at the *exo*-amine may be responsible for loline's toxic properties.[2] There have been multiple experiments performed that display loline's strong insecticidal properties and some studies demonstrate that lolines have comparable toxicity to nicotine. For example, there is evidence that loline alkaloids provide protection to the host from the aphid species *S. graminum* and *R. padi*.[8] Another study proved that loline is toxic to insect larvae of large milkweed bugs (*Oncopeltus fasciatus*).[9] Lolines may also deter feeding on the plant by grubs of Japanese beetles (*Popillia japonica*).[10] In order to fully investigate loline's effects on a variety of insects and mammals an abundance of loline standard must be synthesized.

Previous Syntheses toward loline:

Loline has been a highly sought after synthetic target, but has proven to be a difficult compound to make, which is evident by how few successful syntheses have been described. Two unsuccessful syntheses were published by Glass et al. and Wilson et al. in 1978 and 1981, respectively.[11]   Both syntheses failed when they attempted to add nitrogen through an SN_2 fashion after formation of the tricylic system; therefore, the nitrogen stereocenter cannot be installed with SN_2 inversion. Substitution was unfavorable due to small bond angles and steric hindrance.

Figure 1.3: Failed SN$_2$ nitrogen stereocenter addition

X=OH, Br
Nu: = Ch_3NH_2
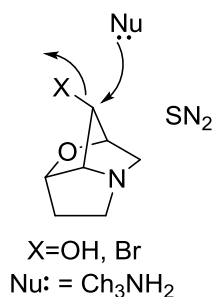
The first successful synthesis of (±) loline was completed in 1986 by Tufariello and coworkers.[12] Taking precedent from syntheses of other pyrrolizidine alkaloids, Tufariello used nitrone-based methodology to construct the pyrrolizidine core (**Scheme 1.1**).   A [3+2] cycloaddition between nitrone **4** and methyl 4-hydroxycrotonate was performed with subsequent hydrogenolysis of the NO bond to arrive to pyrrolizidine **5**.[13] Once the pyrrolizidine skeleton was formed Tufariello had to manipulate the stereochemistry at C1 in **5**, in order to achieve loline's correct stereochemistry of the C3 substituent in **12**.

Scheme 1.1: Tufariello et al. (1986) total synthesis of (±)-loline[12]

Inversion of stereochemistry and functional group transformations
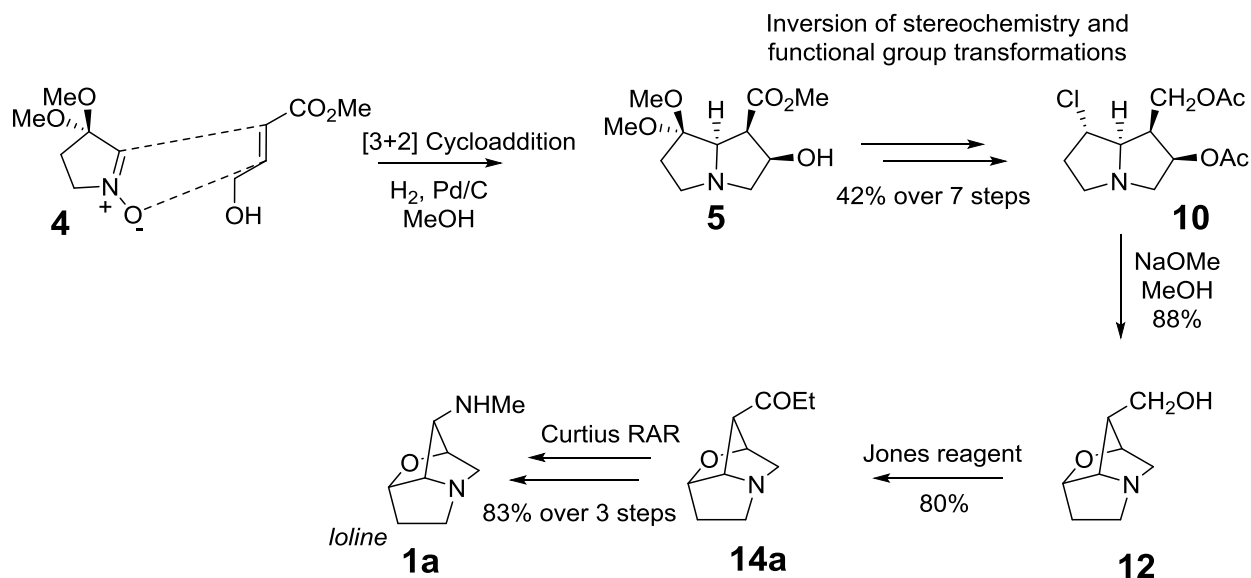
Hydrolysis of **5** caused an unwanted cyclization, but this intramolecular trans ketalization proved that the pyrrolizidine ring system could be closed to achieve the loline skeleton. After protecting the hydroxyl group, Tufariello proceeded through a few transformations to invert the stereochemistry at C1 and C7 before finally arriving to a ring closure that installed the ether bridge in **12**. After oxidation of **12** to yield **14a** Tufariello used methodology based on a Curtius rearrangement to manipulate the C3 hydroxy-methyl moiety. Subsequent reflux with hydrazine hydrate of **14a**, treatment with isoamyl nitrite with HCl, and reduction of the respective carbamate with lithium aluminum hydride yielded *dl*-loline. This route consisted of twelve steps starting from nitrone **4** with a total yield of 24%. Tufariello's use of nitrone cycloaddition as the first step provides a direct route to the pyrrolizidine core, yet he did not install the stereocenters before arriving to the core, which adds more steps.

In 2001 White and coworkers performed the first asymmetric synthesis of (+)-loline.[14] Key steps to his route include an intramolecular [4+2] cycloaddition of an acylnitrosodiene and

Sharpless asymmetric aminohydroxylation (SAA). The route began with commercially available (S)-malic acid **18** and over the next ten steps a 19% overall yield is achieved to afford the protected hydroxamic acid **24** (**Scheme 1.2**). Oxidation of **24** with tetra-*n*-butylammonium periodate resulted in acylnitrosodiene **26**, which then underwent a spontaneous intramolecular [4+2] cycloaddition to give stereoisomeric bicyclic dihydrooxazine **29** and **30** in 57:44. Endo dihydrooxazine **29** is reduced to give an allylic alcohol, which is then mesylated and treated with lithium diisopropylamide. An intermediate metallated lactam cyclized to give dehydropyrrolizidinone **35** with a conveniently placed double bond. In order to obtain the tricyclic skeleton, the double bond of **35** was functionalized with a Sharpless asymmetric aminohydroxylation. Using an added biscinchona alkaloid ligand increased the facial selectivity and regioselectivity of the osmium catalyzed aminohydroxylation to provide **50** and **51** in a modest 3:1 ratio.

Scheme 1.2: White et al. (2001) total synthesis of (+)-loline[14]
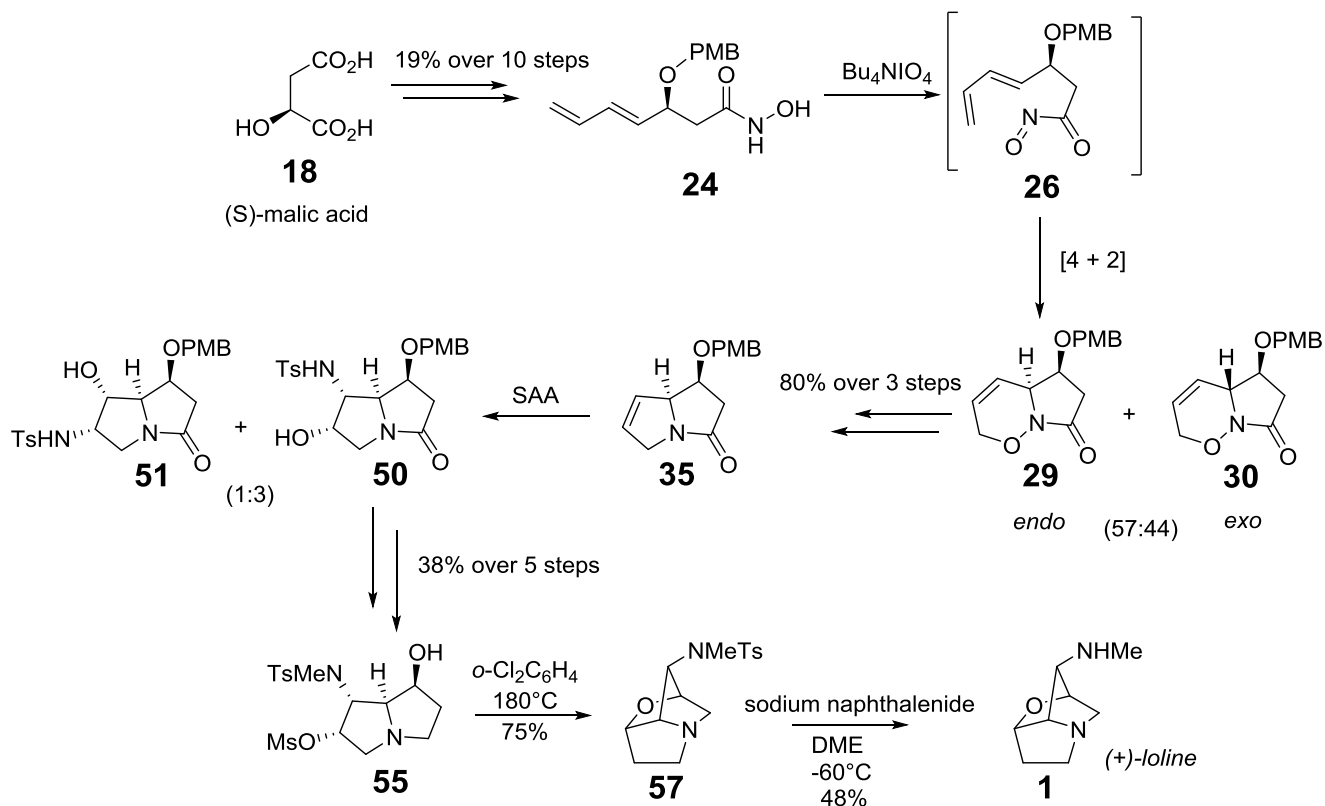
The secondary amino of **50** was then transformed into the *N*-methyl moiety distinctive of loline, and mesylation of the hydroxyl group with subsequent cleavage of PMB created **55**. The C7 hydroxyl group of **55** is in close enough proximity to C2, in order for an effective displacement and subsequent cyclization to achieve the tricyclic loline skeleton. A thermal cyclization occurred using *o*-dichloro-benzene at 180 ℃ to yield *N*-tosylloline **57**. Removal of the tosyl group was completed with sodium naphthalenide, which afforded (+)-loline **1**. This asymmetric synthesis had a total of 22 steps with a total yield of 2.1%. White's synthesis achieves the pyrrolizidine core in 19 steps. One disadvantage of White's route is that he does not make a general loline structure that can be used to generate different loline alkaloids. In addition, White's route has stereoselectivity issues when he used the cycloaddition, regioselectivity

problems with usage of SAA, and elimination concerns during the cyclization, which he overcame using thermal conditions.

In 2011 Scheerer et al. synthesized racemic acetylnorloline using tethered aminohydroxylation (TA) 1st generation conditions.[15] The route began with *N*-Boc-2-azetidinone, which proceeded through a Claisen condensation (**Scheme 1.3**). After decomposition of a diazocarbonyl moiety and N-H insertion, the β-ketoester was reduced then acetylated, which formed two of the four stereocenters. Using a Dieckmann condensation, an enol-lactone was formed, which subsequently underwent a reduction-elimination sequence to transform into an unsaturated lactone. The unsaturated lactone was hydrolyzed and the afforded carboxylate was transformed into as ester with methyl iodide. The intermediate Z-α,β-unsaturated ester went through a functional group transformation to yield primary carbamate **12**. Carbamate **12** served as the TA substrate initially, but when tethered aminohydroxylation 1st generation conditions in the presence of base were first performed a heteroconjugate addition was observed instead to yield **13**.

Scheme 1.3: Scheerer et al. (2011) total synthesis of (±)-loline (1ˢᵗ generation)[15]
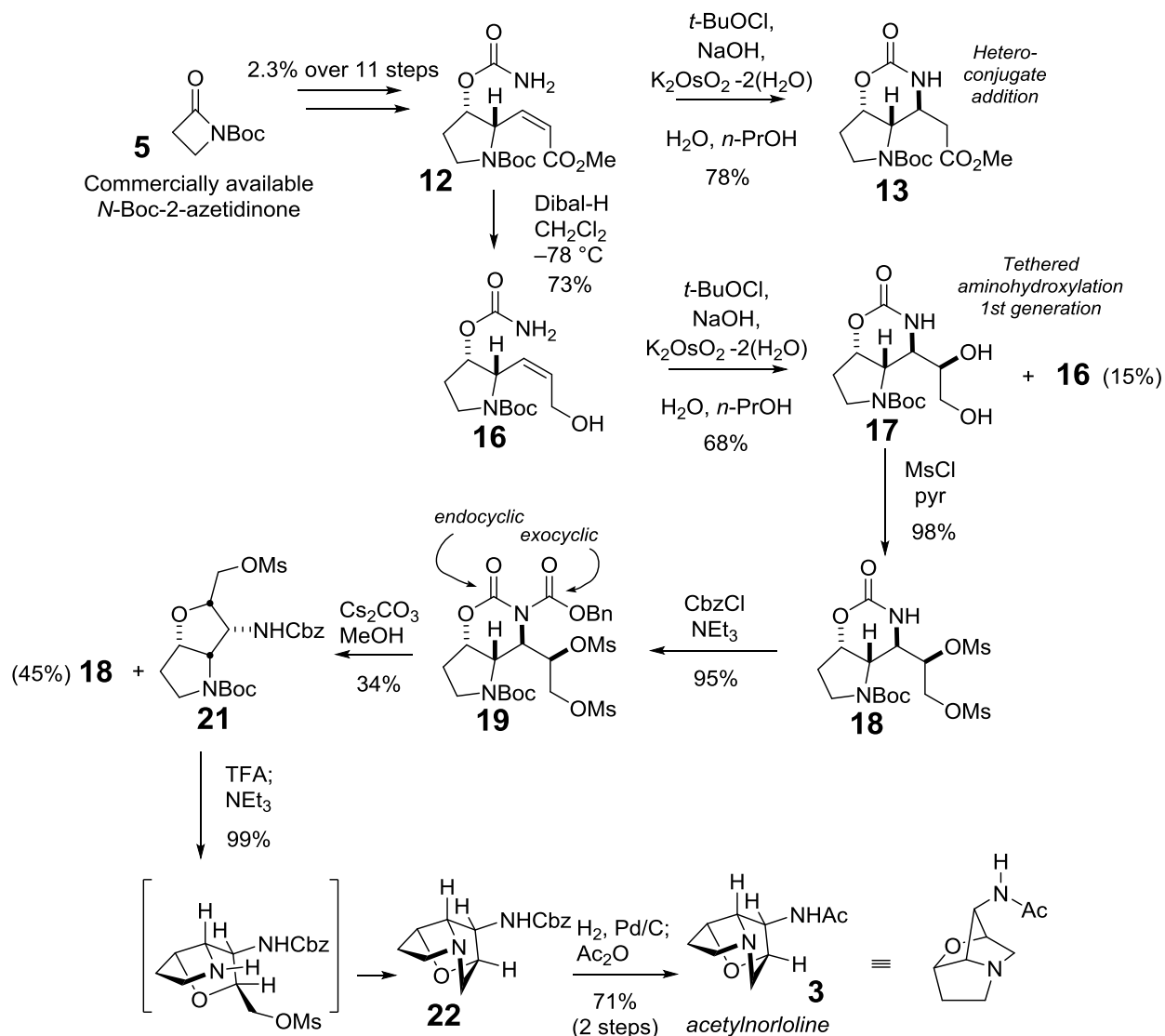
Although unwanted, the β-amino moiety was constructed with high diastereoselectivity, which supported the predicted conformation of TA. Moving forward from **12** required a DIBAL-H reduction of α,β-unsaturated ester to allylic alcohol **16**, which would make the alkene less electrophilic, thus discouraging conjugate addition. Allylic alcohol **16** under TA conditions yielded the desired cyclic carbamate **17** with 68% yield and about 15% of recovered starting material. The four stereocenters were now established and bis-mesylation formed **18** and then

22

reaction with CbzCl and NEt$_3$ generated imide **19**. Methanolysis of **19** resulted in endocyclic and exocyclic cleavages leading to the desired product **21** in 34% yield and formation of **18** again in 45% yield, respectively. The endocyclic intermediate regioselectively attacks the secondary mesylate to form the ethereal bond in **21**. Now the mesylate in **21** is oriented concavely, which will react with the pyrrolidine amine leading to norloline derivative **22**. Acetylnorloline **3** was afforded following hydrogenation and acetylation. Scheerer's synthesis spans 19 steps with a total yield of 2.5%. This synthesis does not create the pyrrolizidine core first, yet goes directly toward the tricyclic skeleton with few alterations to generate acetylnorloline.

Shortly after the Scheerer synthesis Trauner and coworkers published the second asymmetric synthesis of (+)-loline.[16] Key features include a Sharpless asymmetric epoxidation (SAE), a ring closing metathesis, and an unprecedented transannular aminobromination. His route commences with an enantiotopos and diastereoface-selective Sharpless epoxidation on achiral divinyl carbinol **7** to afford epoxide **8** (**Scheme 1.4**). Nucleophilic attack of 3-butenylamine **9** and subsequent protection of the nitrogen with a Cbz group yielded diene **10**. A ring closing metathesis with Grubbs 2nd generation catalyst is performed on diene **10** to generate eight-membered ring **11** with a diol. After activating the diol an SN$_2$ reaction occurred to give **13**. Next, Trauner used a unique transannular nucleophilic substitution (**Scheme 1.5**). First, **13** was activated with bromine to form a brominium ion, which allowed the carbamate nitrogen to attack the electrophilic carbon to form *N*-acylammonium ion. The Cbz group is cleaved by methanol and the pyrrolizidine skeleton **14** is constructed.
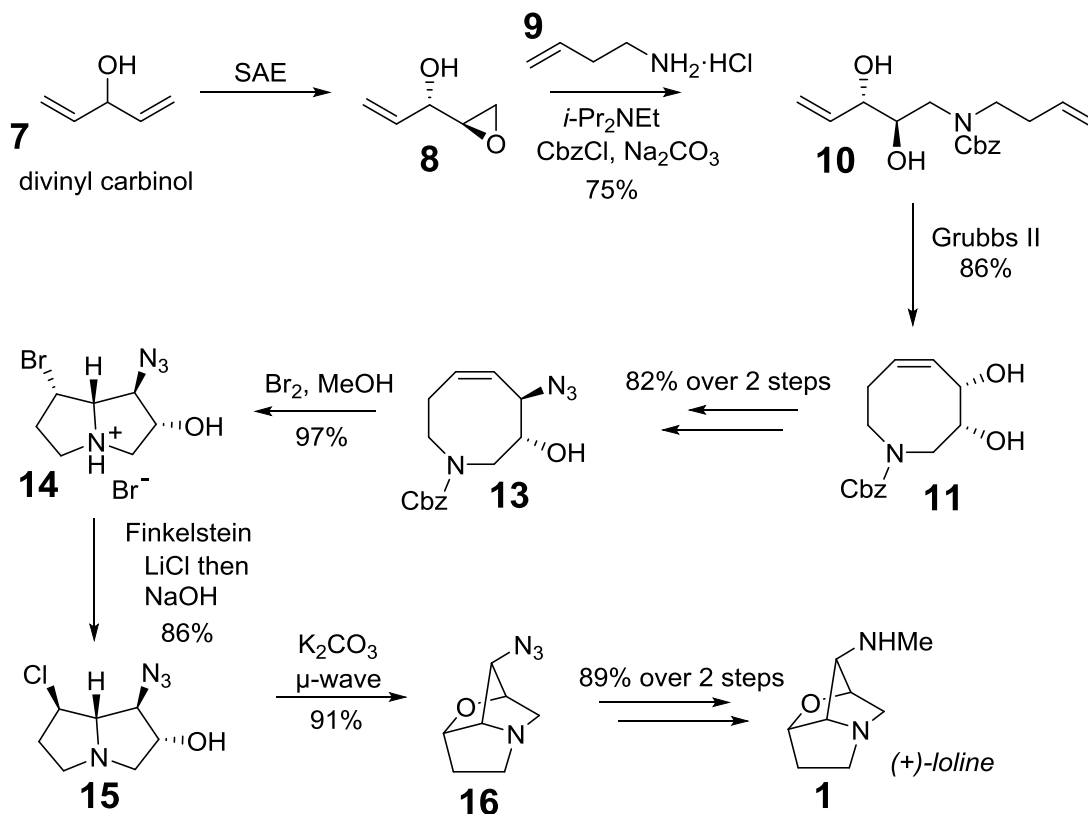
Using the Finkelstein reaction, the inversion of the stereocenter at C7 afforded **15**. Heating **15** in a microwave with potassium carbonate led to a 5-*exo*-tet ring closure, thus establishing the ether bridge and formed azide **16**, which could lead to a variety of loline alkaloids. To arrive to (+)-loline **1**, azide **16** was hydrogenated with di-t*ert*-butyl pyrocarbonate, which was then reduced with lithium aluminum hydride.

Scheme 1.5: Trauner et al. transannular nucleophilic substitution with brominium ion[16]
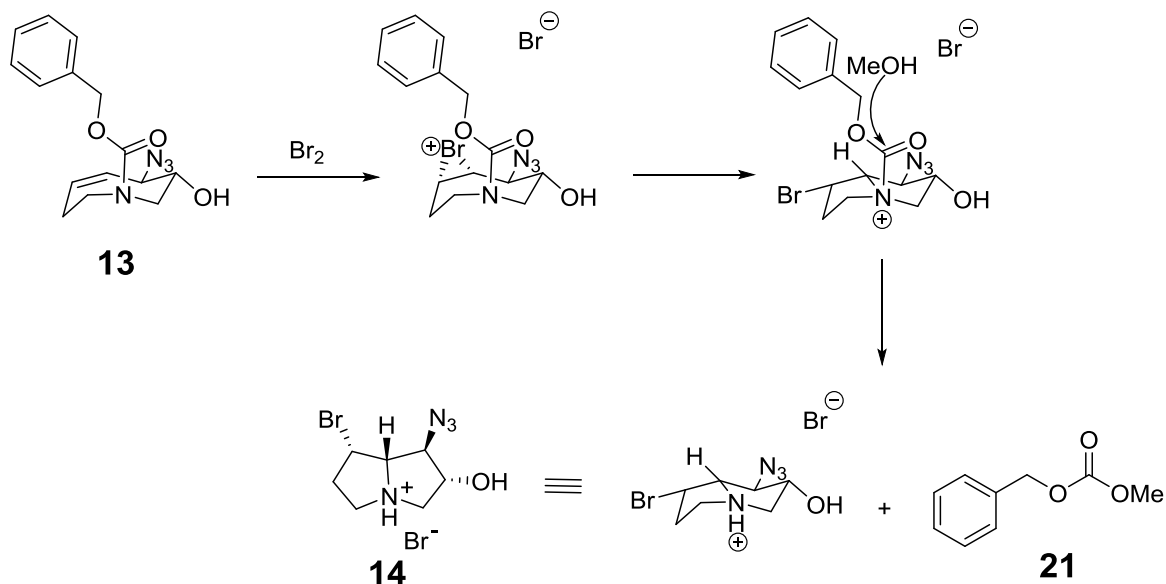
Trauner's asymmetric route is completed in 10 steps with a total yield of 35%. His route proves most efficient with only seven steps to generate the pyrrolizidine core and three subsequent steps to yield (+)-loline. In addition, there is only one protecting group used throughout the route, yet it does not require cleavage because it is strategically lost during a bond formation.

Conclusion:

The syntheses of loline discussed proved successful in generating loline, but Trauner's route is the most efficient (**Table 1.1**). In addition, only Scheerer and Trauner yield a loline intermediate that can lead to different loline alkaloids. Scheerer 1st generation synthesis had problems with regioselectivity and stereoselectivity. Furthermore, creating great quantities of the loline alkaloids for biological testing from this synthesis is not realistic. The 2nd generation synthesis builds upon the 1st generation, but addresses the issues raised in the 2011 synthesis. The 2nd generation synthesis improves regioselectivity and stereoselectivity, while providing a shorter route.

Table 1.1: Comparison of current loline total syntheses

Author	Year	Steps	Total Yield	Stereoisomerism
Tufariello	1986	12	24%	racemic
White	2001	22	2.1%	asymmetric
Scheerer 1st	2011	19	2.5%	racemic
Trauner	2011	10	35%	asymmetric

References:

1. Nicolaou, K.C.; Sorensen, E.J. *Classics in Total Synthesis: Targets, Strategies, Methods*; VCH: New York, 1996; pp. 1-18.
2. Schardl, Christopher L.; Grossman, Robert B.; Nagabhyru, Padmaja; Faulkner, Jerome R.; Mallik, Uma P. *Phytochemistry* **2007**, *68*, 980-996.
3. Gundel, Pedro E.; Pérez, Luis I.; Helander, Marjo; Saikkonen, Kari. *Trends in Plant Sci.* **2013**, *18*, 420-427.
4. Siegel, Malcom R.; Bush, Lowell P. *Phytochemical diversity and redundancy in ecological interactions*; New York, 1996; pp. 81-119.
5. Schardl, Christopher L.; Leuchtmann, Adrian; Spiering, Martin J. *Annu. Rev. Plant Biol.* **2004**, *55*, 315–340.
6. Conover, Michael R.; Messmer, Terry A. *Condor* **1996**, *98*, 859-862.
7. Fuchs, B.; Krischke, M.; Mueller, M. J.; Krauss, J. *J. Chem. Ecol.* **2013**, *39*, 1385-1389.
8. Wilkinson, H. H; Siegel, M. R.; Blankenship, J. D.; Mallory, A. C.; Bush, L. P.; Schardl, C. L. *MPMI* **2000**, *13*, 1027-1033.
9. Yates, S. G.; Fenster, J. C.; Bartelt, R. J. *J. Agric. Food Chem.* **1989**, *37*, 354-357.
10. Patterson, C. G.; Potter, D. A.; Fannin, F. F. *Entomologia Experimentalis et Applicata* **1991**, *61*, 285-289.
11. Glass, R. S.; Deardorff, D. R.; Gains, L. H. *Tetrahedron Lett*. **1978**, 2965-2968. b) Wilson, S. R.; Sawacki, R. A.; Huffman, J. C. *J. Org. Chem*. **1981**, *46*, 3887-3891.
12. Tufariello, J. J.; Meckler, H.; Winzenberg, K. *J. Org. Chem.* **1986**, *51*, 3556-3557.
13. Tufariello, J. J.; Lee, G. E. *J. Am. Chem. Soc.* **1980**, *102*, 373-374.
14. Blakemore, P. R., Kim, S. K., Schulze, V. K., White, J. D., & Yokochi, A. F. *J. Chem. Soc., Perkin Trans. 1* **2001**, 1831-1847.
15. Hovey, M. T.; Eklund, E. J.; Pike, R. D.; Mainkar, A. A.; Scheerer, J. R. *Org. Lett.* **2011**, *13*, 1246-1249.
16. Cakmak, M., Mayer, P.; Trauner, D. *Nat. Chem.* **2011**, *3*, 543-545.
17. Fraenkel, G. S. *Science* **1959**, *129*, 1466-1470.
18. Stamp, N. *Q. Rev. Biol.* **2003**, *78*, 23-55.
19. Gwinn, K. D.; Collins-Shepard, M. H.; Reddick, B. B. *Phytopathology* **1991**, *81*, 747-748.
20. Craven, K.D.; Blankenship, J.D.; Leuchtmann, A.; Hignight, K.; Schardl, C.L. *Sydowia* **2001**, *53*, 44–73.
21. Klotz, J. L.; Kirch, B. H.; Aiken, G. E.; Bush, L. P.; Strickland, J. R. *J. Anim. Sci.* **2009**, *87*, 2437-2447.

CHAPTER II

PROGESS TOWARD SYNTHESIS OF ASYMMETRIC LOLINE ALKALOIDS

Introduction:

Following strong precedent from Scheerer 2011 synthesis, we began working on the second generation route to synthesize enantiopure loline alkaloids. The second generation synthesis is composed of 11 enantioselective steps to the TA substrate. The first generation did not provide enough material for fully researching the activities of loline alkaloids, its potential as a natural pesticide, or the host-fungal-insect relationships. The second generation synthesis aims to provide the significant quantities needed. During the methanolysis in the first generation a mixture of the endocyclic and exocyclic cleavage occurred when loss of the Cbz moiety reverted to **18** (**Scheme 2.1**). However, during an experiment Scheerer found that when Boc functionality replaced Cbz moiety, reversion

Carboxybenzyl (Cbz)

to **18** did not occur and the desired secondary alcohol was formed more competitively with 80% yield. Therefore, a Boc-derived imide was used.
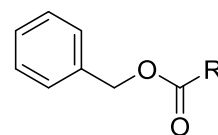
Scheme 2.1: Comparison of nitrogen protecting groups during cyclization
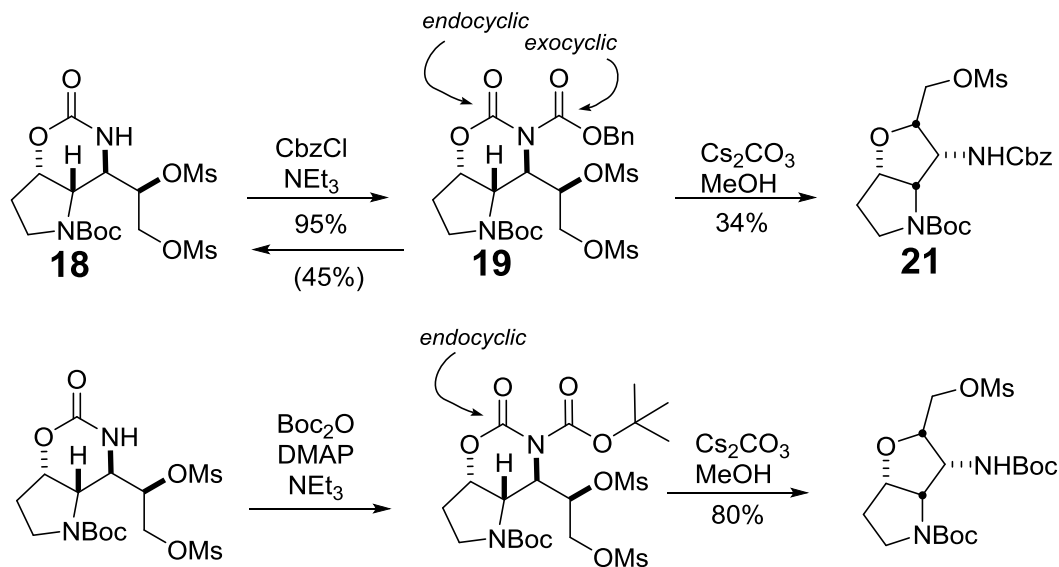
Analyzing the retrosynthesis of Scheerer 2nd generation of loline allows us to address the similarities and main revisions when compared to the first generation (**Scheme 2.2**). Starting with the loline-Boc derivative, the preceding steps toward the cyclic carbamate remain the same except for the nitrogen protecting group during methanolysis. Arriving to the cyclic carbamate, TA substrate, and methyl ester carbamate follow precedent from the first generation. However, one change involves usage of ring closing metathesis (RCM) to arrive to the cyclic lactone. An acylation will be used to afford the diene. Preceding the acylation is the Petasis borono-Mannich (PBM) addition with the installation of a new stereocenter. To achieve the PBM substrate requires cyclization, lithiation, protecting group addition, and reduction from the starting material. Another major change from the previous synthesis includes changing the *N*-protecting group from Boc to Cbz for better regioselectivity during the final cyclization toward the tricyclic loline core and for the strong Lewis acidic conditions of the *N*-acyliminium PBM addition. In addition, the starting material is chiral, therefore allowing an asymmetric synthesis to be completed. Key reactions of the route include TA, PBM, and RCM.

Scheme 2.2: Retrosynthetic analysis of Scheerer 2nd generation synthesis of loline
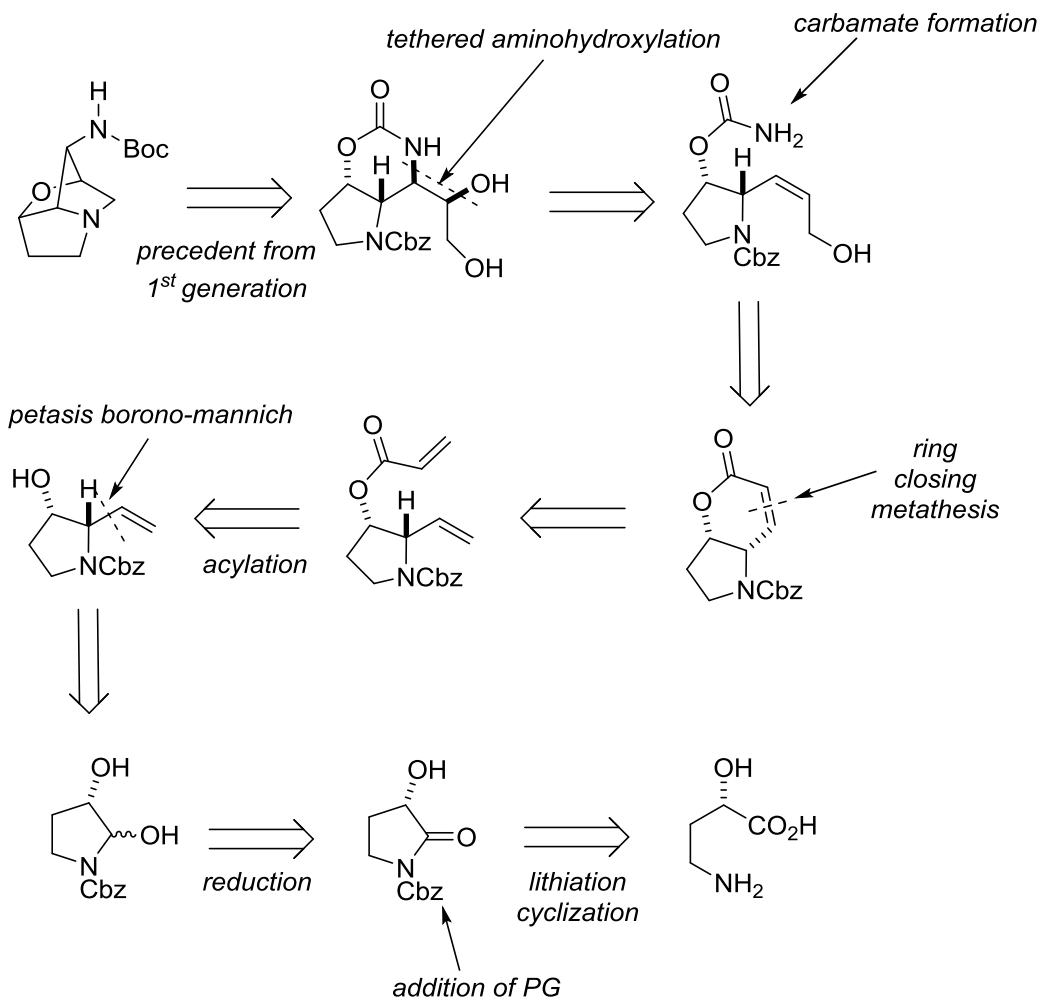
Tethered Aminohydroxylation Background:

Before the tethered aminohydroxylation method was discovered by Donohoe, the Sharpless asymmetric aminohydroxylation, first introduced in 1996, was commonly used to prepare stereospecific vicinal amino alcohols with an osmium catalyst.[1] With addition of a ligand, asymmetric induction is possible. For example, a carbamate will provide the nitrogen source and *t*-butyl hypochlorite acts as the stoichiometric oxidant in the presence of potassium osmate and chinchona alkaloids to yield an amino alcohol. This method was utilized in the White synthesis described earlier.

The reaction has been theorized to go through two simultaneous catalytic cycles (**Scheme 2.3**).[2] The primary cycle commences with the nitrogen oxidizing agent acting upon the Os (VI) species to yield the omidotrioxoosmium (VIII). This species proceeds through a cycloaddition to the alkene with reinforced enantio- and regioselectivity by the chiral ligand, which results in the azaglycolate complex. At the same time the oxidized azaglycolate may enter the ligand-free secondary cycle if it goes through an addition to the second alkene to yield bis(azaglycolate)osmium species before hydrolysis happens. In the secondary cycle low enantio- and regioselectivity is observed due to the absence of the chiral ligand.

Scheme 2.3: AA Catalytic Cycles[2]

high enantioselectivity

hydrolysis

Primary Cycle

oxidation

Secondary Cycle

addition

addition

hydrolysis

low enantioselectivity

L=ligand
R=SO$_2$R, COOR, etc.
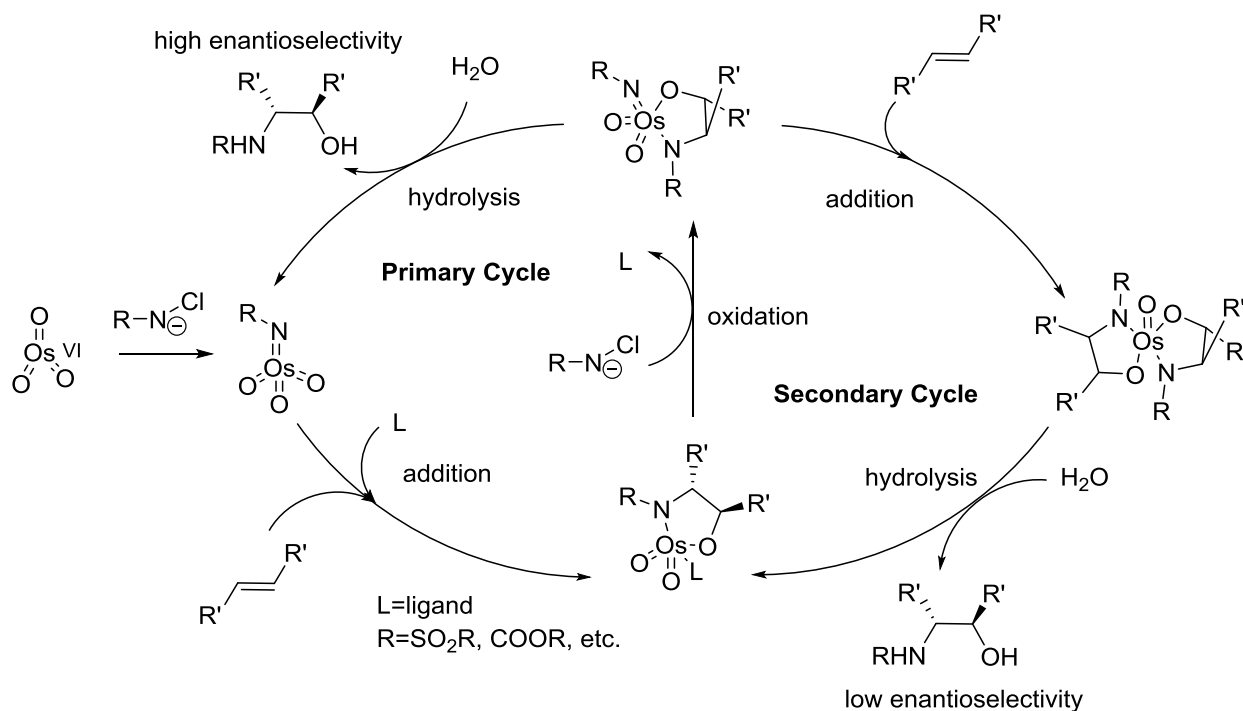
Since Sharpless aminohydroxylation lacks regiochemistry when unsymmetrical alkenes are applied, Donohoe expanded upon AA and created tethered aminohydroxylation (TA). TA overcomes regioselectivity issues by tethering the source of nitrogen to an achiral allylic alcohol, which controls the regiochemistry.[3] Donohoe's first generation conditions debuted in 2001. TA includes an osmium catalyst and *t*-butyl hypochlorite as the oxidant. First, the nitrogen of the carbamate is deprotonated by NaOH then oxidized by *t*-butyl hypochlorite. Next, the oxidized chlorinated nitrogen oxidizes potassium osmate to the osmium tetroxide analogue. Then the osmium tetroxide adds to the alkene, which becomes azaglycolate osmate ester. This ester is then oxidized and hydrolyzed during the course of the reaction. Disadvantages of the first generation include low yields, poor reaction of homoallylic alcohols, and poor reaction of 5-membered rings with endocyclic alkenes. Furthermore, chlorination of the alkene is a common

competing side reaction that leads to lower yields since the chlorinated nitrogen can prove unstable to the reaction conditions.[4]

Tethered aminohydroxylation 2nd generation conditions debuted in 2006.[5] The main difference between the first and second generation is functionalizing the carbamate into a form able to directly oxidize the osmium catalyst. As a result, *t*-butyl hypochlorite can be avoided. Additionally, there is no longer a need for base because the need to deprotonate in order to add *t*-butyl hypochlorite is absent. In the second generation, Donohoe uses *N*-sulfonyloxycarbamates as a reoxidant, which is added onto a hydroxylamine before the aminohydroxylation. As a result there is complete conversion, lower catalyst loading, and yields are increased. Furthermore, primary allylic carbamates and homoallylic alcohols are competitive substrates. However, some disadvantages include the low stability and short shelf-life of *N*-sulfonycarbamate and the reaction is sometimes capricious.

In 2007 Donohoe made improvements to TA and published TA 3rd generation conditions.[6] Similar to the second generation conditions in that functionalized carbamate oxidizes the catalyst except aroyloxycarbamates are used. The third generation protocol increases yields even more and offers a more predictable reaction. In addition, aroyloxycarbamates are more stable and can be stored for several weeks. Other improvements upon the previous generation include *anti* selectivity for homoallylic carbamates, *syn* selectivity for allylic carbamates and decreased catalyst loading to 1 mol %. A comparison between the first, second and third generation conditions of TA is shown in **Scheme 2.4**.

Scheme 2.4: Comparison between TA 1st, 2nd, and 3rd generation protocols[4]
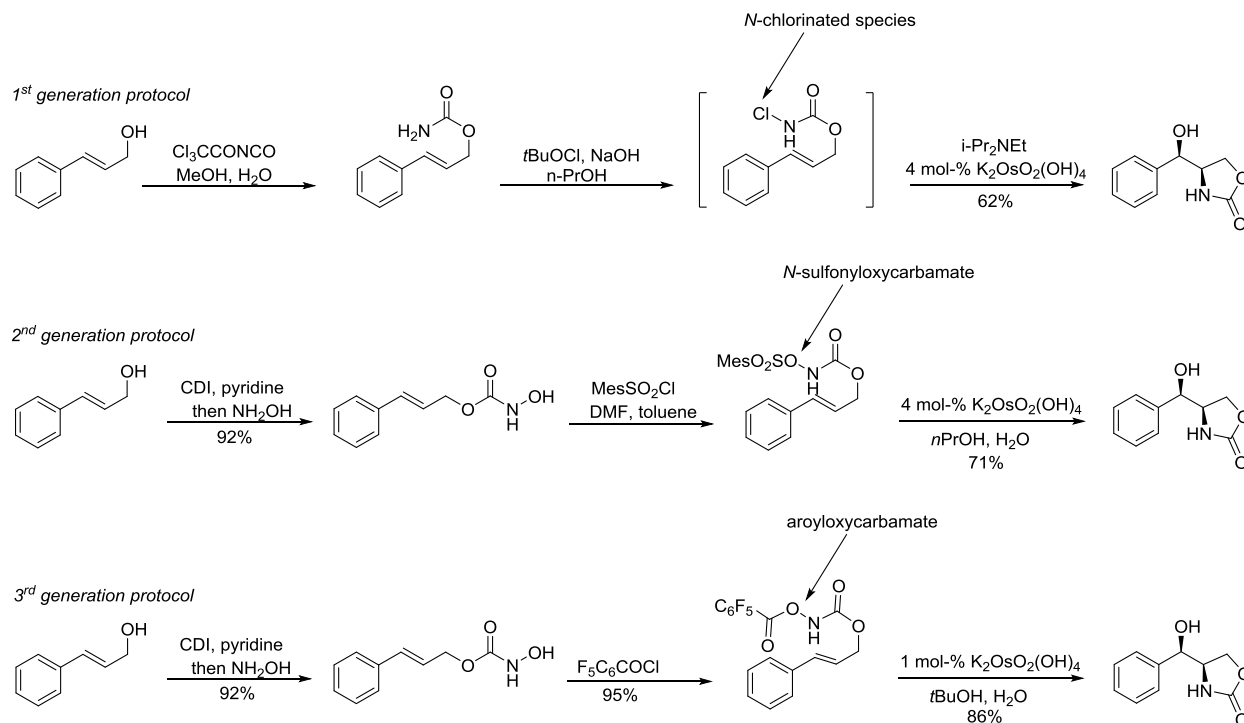
The hypothesized mechanism for TA 2nd and 3rd generation is similar to the Sharpless AA cycles mentioned earlier. First, *N*-oxy-carbamate **63** oxidizes osmium (VI) to form trioxoimido osmium(VIII) complex **64** (**Scheme 2.5**).[4] **64** goes through an intramolecular [3+2] cycloaddition onto the alkene to form osmium(VI) azaglycolate **65**, which was verified through an X-ray crystallographic analysis of **69**. A second molecule **63** rapidly reoxidizes osmium(VI) species **65** to generate osmium(VIII) species **66**. If hydrolysis of **66** occurs more quickly than another cycloaddition then **66** enters the primary cycle. However, there is reason to believe that TA of allylic carbamates reacts through the secondary cycle and cycloaddition of the osmium species to the tethered olefin is faster than hydrolysis.

Scheme 2.5: TA Catalytic Cycles[4]

Primary Cycle

intermolecular
hydrolysis
slow

Secondary Cycle

intramolecular
addition
fast

(±)-**67**

H₂O

(±)-**66** Os^VIII

(±)-**68** Os^VI

63

64 Os^VIII

R=SO₂Ar, COAr

Os^VI

(±)-**65** Os^VI

(±)-**67**

H₂O

(±)-**69** Os^VI

1 equiv. K₂OsO₂·2(H₂O)
1 equiv. TMEDA
nPrOH
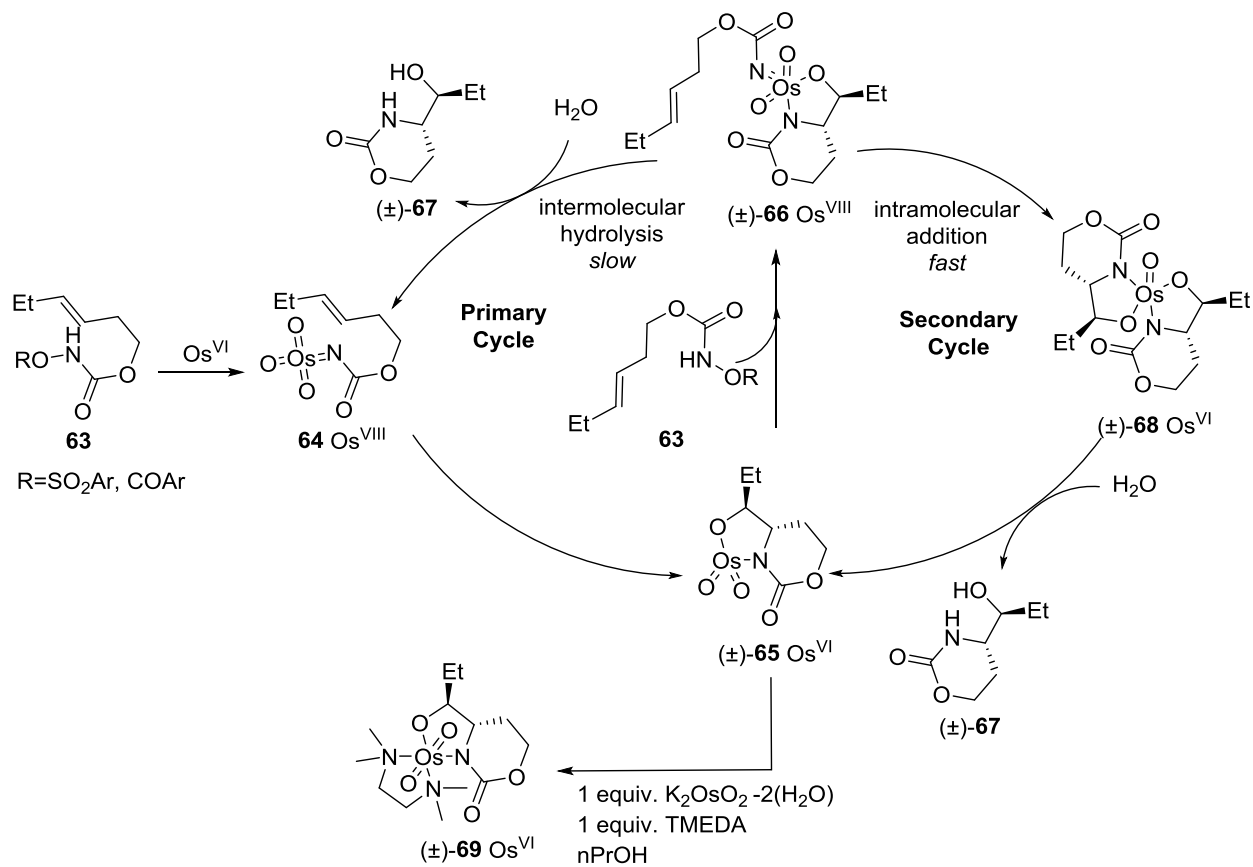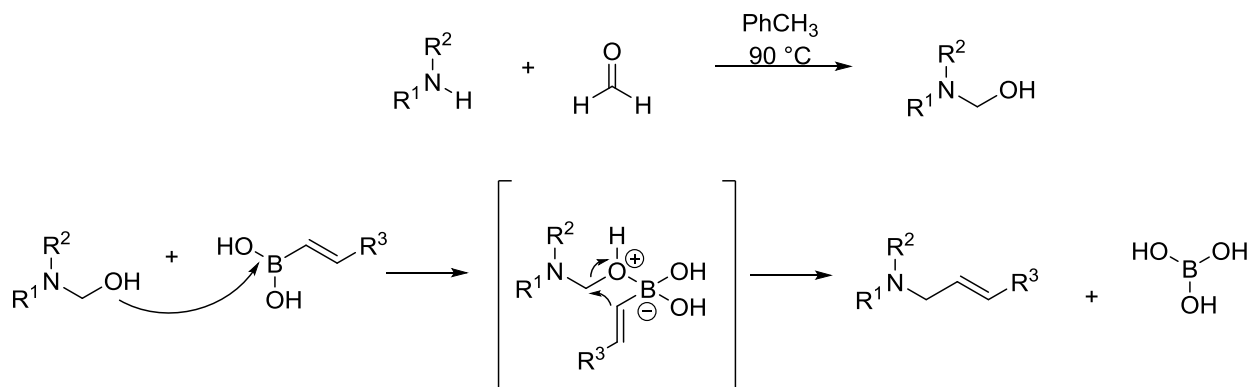
Petasis borono-Mannich Background:

In 1993 Petasis et al. showed that the reaction of vinyl boronic acids after addition of secondary amines and paraformaldehyde generates tertiary allylamines with geometry intact.[16] This new reaction became known as the Petasis borono-Mannich addition. Addition of the carbonyl and amine forms α-hydroxy amine (**Scheme 2.6**). Then the hydroxyl group attacks the electrophilic boron to form an "ate"-complex. In this intramolecular vinyl transfer the *E*-geometry in the boronate is preserved in the newly formed allylic amine. In addition, aldehyde substrates with α-hydroxyl groups can help vinyl transfer.

Scheme 2.6: General reaction conditions for classic Petasis borno-Mannich addition[16]

In 1999 Batey et al. created a variant of the Petasis borono-Mannich addition and demonstrated that vinyl boronates could undergo nucleophilic addition to an *N*-acyliminium ion formed *in situ*.[7] In the presence of Lewis acid (boron trifluoride etherate) addition is successful and alkene geometry of the boronate is maintained in the product. The mechanism for PBM is still not fully understood, but it is thought that given the necessity of the Lewis acidic conditions an *N*-acyliminium ion is formed. The boronate attacks *N*-acyliminium ions exclusively from the β-oxygen face through boron-oxygen coordination (**Scheme 2.7**). Similar to the classic PBM

addition olefin geometry from the boronate is retained when addition to the ion occurs. This

reaction will be used as a precedent in our synthesis since a new stereocenter is formed.

Scheme 2.7: Petasis borono-Mannich addition mechanism of *N*-acyliminium ion[7]
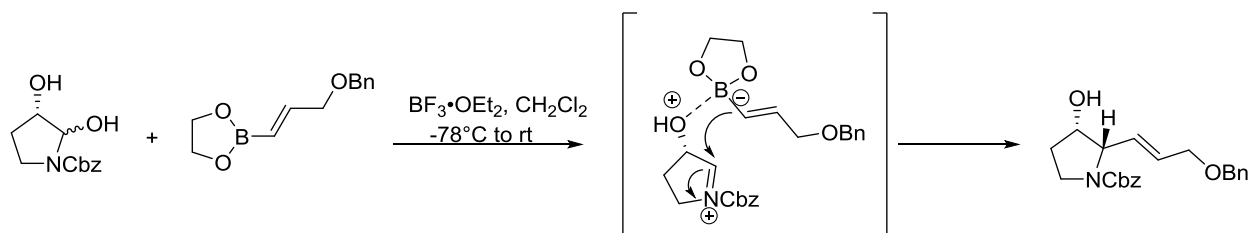
Furthermore, boronic acid or ester derivatives have great water and air stability, low toxicity, and

other functional groups tolerate them. This novel methodology of additions using organoboronic

acids or esters proves useful for synthesizing alkaloids; thus, it is incorporated into our synthesis.

Ring Closing Metathesis using Grubb's Catalysts:

Ring closing metathesis is a powerful synthetic method to forge two olefins in order to create a ring. In 1995 Robert Grubbs introduced ruthenium-based alkylidenes, which became known as Grubb's catalysts.[8] Grubb's catalysts have five ligands attached to ruthenium, which include two neutral electron-donating groups (*e.g.*, trialklphosphines), two monoanionic groups (*e.g.*, halides), and one alkylidene substituent (*e.g.*, unsubstituted and substituted methylidenes).[9]

Figure 2.1: Structures of different Grubb's catalysts

Grubbs 1ˢᵗ Generation   *Grubbs 2ⁿᵈ Generation*   *Hoveyda-Grubbs 2ⁿᵈ Generation*
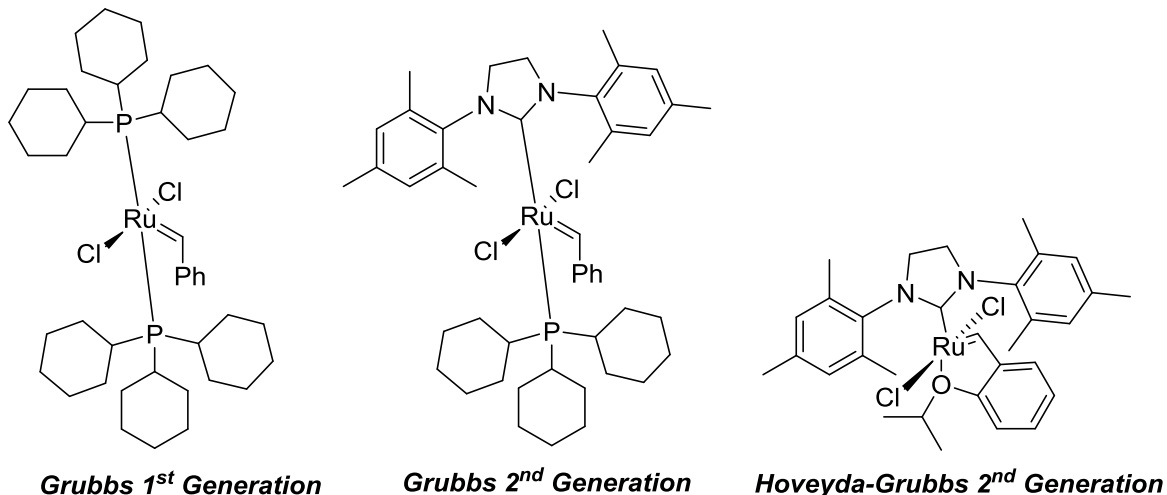
The first generation and second generation catalysts differ in their neutral ligands (**Figure 2.1**). The first generation catalysts have great functional-group tolerance. Additionally, they perform poorly when RCM is applied to tri- and tetrasubstituted cycloalkenes and CM of sterically hindered or electron deficient alkenes. The debut of second generation catalysts in 1999 addresses these issues while still maintaining the advantages of the first generation catalysts. Also, the Grubb's second generation catalysts initiate more slowly than the first generation ones, so increased temperatures are needed for slower initiations. Their increased reactivity stems

from the ability to coordinate the alkene in the presence of free phosphine better than the first generation catalysts. One disadvantage of both is air-sensitivity issues. Variants of the Grubb's catalysts, like Hoveyda-Grubb's catalysts, have been generated to improve reactivity. The mechanism of RCM involves the ruthenium-based catalyst binding in this case to one of the terminal alkenes to form ruthenacyclobutane, which then undergoes a cycloreversion to remove ethene and forms a ruthenium carbene complex (**Scheme 2.8**). Ruthenacyclobutane is formed again with the second olefin. Collapse of the metallacyclobutane yields formation of the desired ring, as shown in **7**.

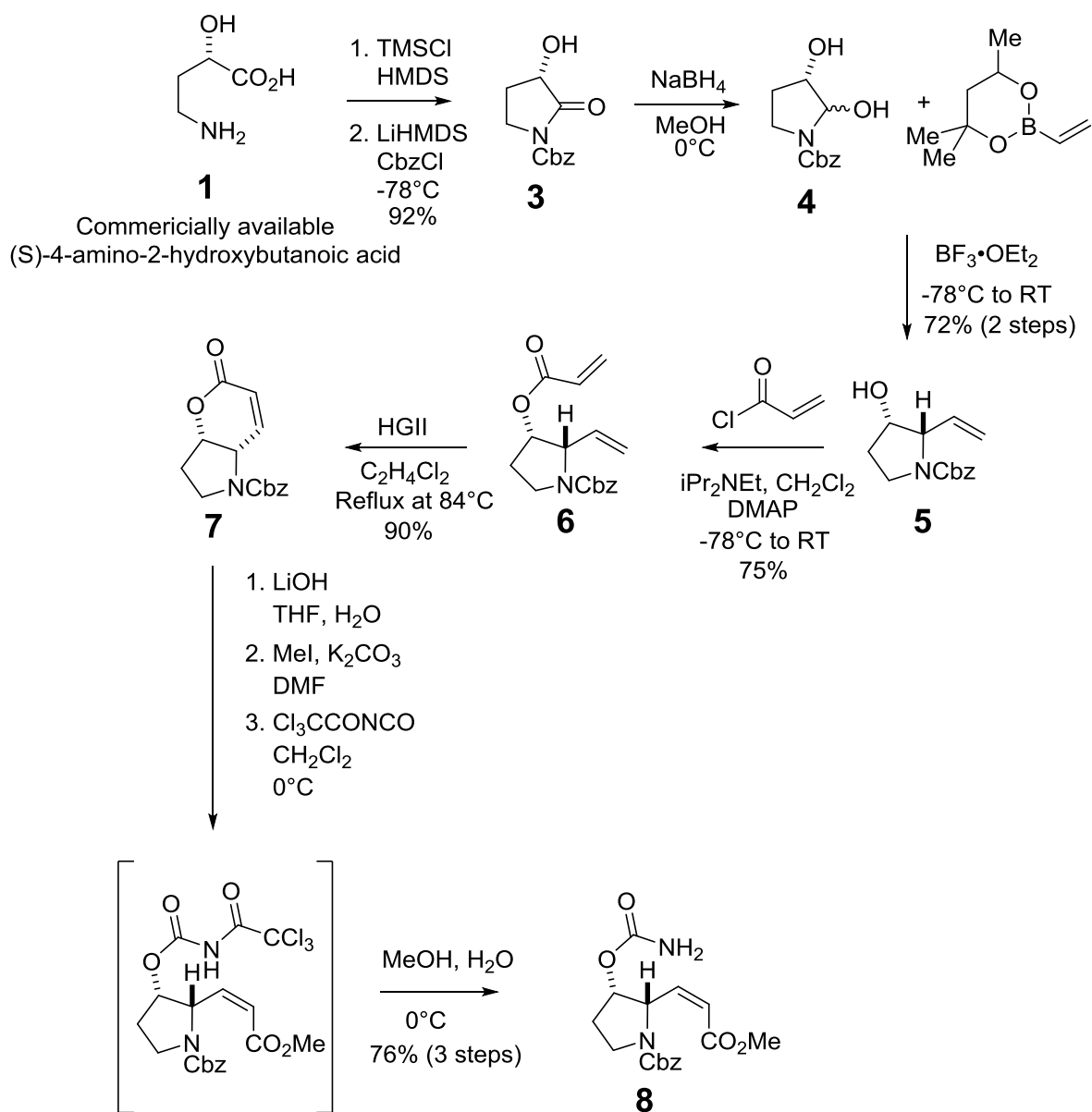**Scheme 2.8: Mechanism of RCM using Grubb's catalyst**
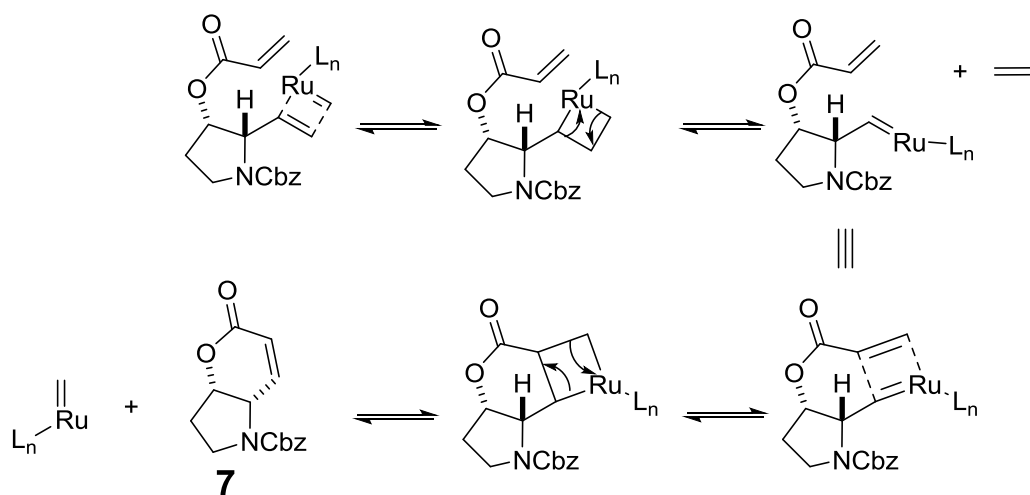
Methods and Results:

The route toward the TA substrate starts with purchased chiral substrate,

(*S*)-4-amino-2-hydroxybutanoic acid **1** (**Scheme 2.9**).

Scheme 2.9: Synthetic route toward α,β-unsaturated ester

Amino acid **1** goes through a cyclization after exposure to TMSCl, excess HMDS, and refluxing xylene to generate pyrrolidine **2**. The amide nitrogen of **2** is lithiated using LiHMDS at -78 °C, so that a regioselective addition of CbzCl afforded protected lactam **3**. Protected lactam **3** is reduced using sodium borohydride to yield diol **4**. Petasis borono-Mannich addition may be performed on **4** to generate diastereomeric allylic pyrrolidine **5**. Precedent by Batey and coworkers of the ethylene glycol boronate (**Scheme 2.7**) was used. In our route we use 2-methyl-2,4-pentadiol derived boronate. These boronate derivatives are stable and are as reactive as the precedent. The required adjacent hydroxyl group directs stereospecific nucleophilic attack of the vinyl boronate to the *N*-acyliminium ion (**Scheme 2.10**).[10]

<p align="center">**Scheme 2.10: PBM intermediate**</p>
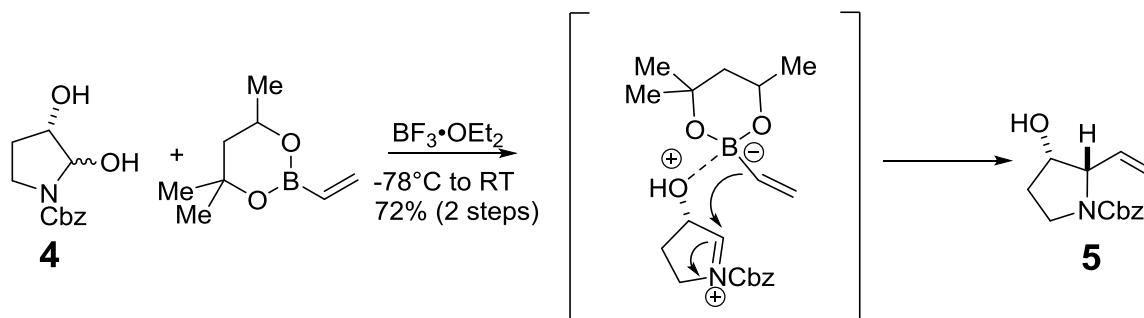
With another stereogenic center established, acylation with acryloyl chloride was performed to establish acrylate pyrrolidine **6**. With two alkenes in place, we could perform a ring closing metathesis to form cyclic lactone **7**. Trials with Grubb's 1st and 2nd Generation catalysts failed to produce high yields (**Table 2.1**). Initially, we used Grubb's II in toluene heated to 80 °C. Catalyst loading originally began with 4 mol %, but was added twice more during the course of the reaction to force the reaction proceed. Using this catalyst yielded 50% conversion. We used Grubb's I under the same conditions, but only observed 5% conversion. Next, utilization of RCM with Hoveyda-Grubb's II proved the most effective due to its more reactive nature with electron deficient substrates.[11] At first, using HGII in dichloroethane in an

88 °C oil bath gave 40% conversion. The conversion was further improved to 100% with particular attention to anhydrous and inert conditions (degassing multiple times and alterations in equipment) and refluxing the reaction solution for 5-10 minutes before adding the catalyst.

Table 2.1: Comparison of RCM catalysts

Catalyst	Conditions	Loading	Conversion
Grubb's I	PhMe, 80 °C	12% (3x4%)	ca 5%
Grubb's II	PhMe, 80 °C	12% (3x4%)	50%
Hoveyda-Grubb's II	DCE, 84 °C	5%	100%

Opening of cyclic lactone **7** to the unsaturated ester was accomplished with saponification using lithium hydroxide. A subsequent esterification with MeI was performed on the intermediate carboxylic acid. Use of trichloroacetyl isocyanate generated an imide intermediate and subsequent hydrolysis yielded methyl ester carbamate **8**. Synthesis of **8** resulted in Z-geometry olefin, which is necessary preparation for the upcoming tethered aminohydroxylation.

Although there was precedent from the 2011 synthesis, we ran into issues when reducing α,β-unsaturated ester **8** to allylic alcohol **9** (**Scheme 2.11**).

Scheme 2.11: Synthesis toward TA substrate
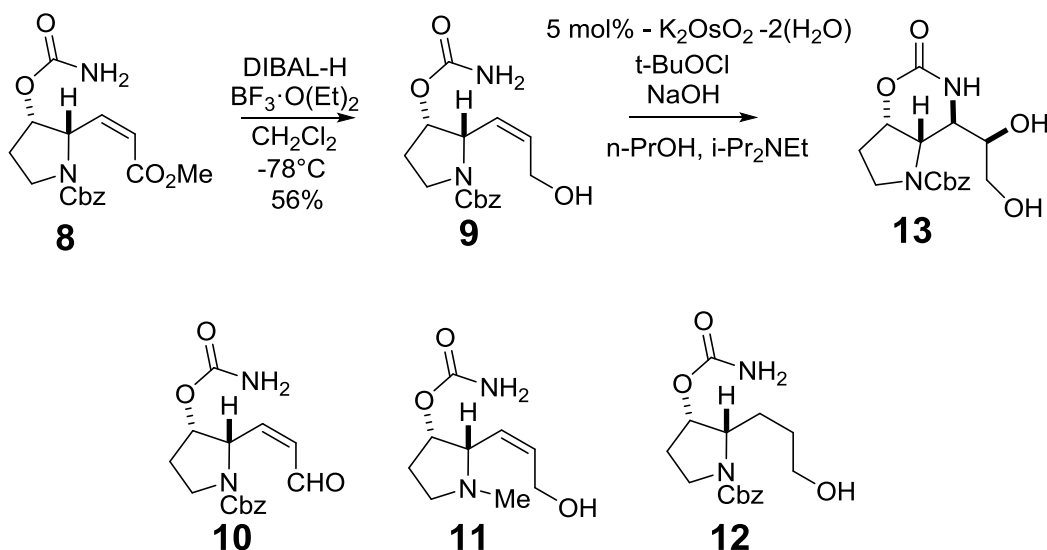
The conditions from Scheerer 1st generation were DIBAL-H at -78 °C with a yield of 73%, but when applied to the 2nd generation synthesis results were not the same (**Table 2.2**). There was poor crude mass recovery and significant amounts of aldehyde **10** due to a partial reduction since a stable tetrahedral intermediate was formed. Next we warmed the reaction from −78 °C to −40 °C, in order to collapse the aluminum tetrahedral intermediate and further reduce to the alcohol, but *N*-Cbz was reduced to methyl amine **11**. We started to investigate different hydride reducing agents; therefore, $NaBH_4$ in combination with $CeCl_3 \cdot 7H_2O$ as a mild, selective 1,2-reducing agent seemed attractive.[12] We tried this combination, but no reaction occurred. Lithium borohydride is more reactive than sodium borohydride, but less reactive than DIBAL-H and $LiAlH_4$.[13] Reduction with $LiBH_4$ performed a conjugate addition and gave only saturated alcohol **12**. After the realization that reduction of α,β-unsaturated ester to allylic alcohols using borohydrides was not favored since conjugate reduction was faster we returned to aluminum-based hydride reductants.[14] Next we used $LiAlH_4$ at −78 °C, which had low conversion and gave

less than 5% yield of **9**. We thought that allowing the reaction to slowly warm to −10 °C might increase the rate of conversion, but this gave a 26% yield of **9**, 22% yield of **12**, and recovered starting material. Then we attempted the reduction with LiBEt$_3$H$_3$, also known as superhydride, which is a more reactive reducing agent than LiAlH$_4$. Complete conversion was not achieved with only a 16% yield of **9**. However, the yield of **12** did decrease to less than 5%. Finally, we considered DIBAL-H in combination with BF$_3$·O(Et)$_2$ as a Lewis acid catalyst. DIBAL-H in combination with this Lewis acid acts as a selective 1,2-reduction of α,β-unsaturated esters to yield allylic alcohol **9** in 56% yield.

Table 2.2: Comparison of hydride reductants
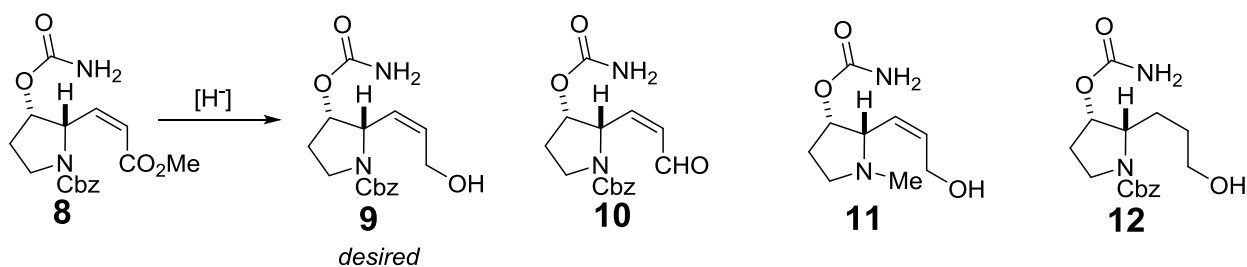
Reductant	Conditions	Reaction time (hr.)	Product	Yield
DIBAL-H	-78 °C	1	N-Boc allylic alcohol	73%
DIBAL-H	-78 °C	1	10 (9 minor)	35%
DIBAL-H	-78 °C → -40 °C	1	11 (9 minor)	20%
NaBH$_4$	CeCl$_3$·7H$_2$O, MeOH, 0°C	2.5	NR	NR
LiBH$_4$	THF, -78 °C → rt	17	12	n.d.
LiAlH$_4$	THF, -78 °C	1	9	5%
LiAlH$_4$	THF, -78 °C → -10 °C	3	9 12 8	26% 22% 15%
LiBEt$_3$H	THF, -78 °C → -40 °C	3.5	9 12 8	16% <5% 15%
DIBAL-H	BF$_3$·OEt$_2$, CH$_2$Cl$_2$, -78°C	0.5	9	56%

Also modeling after Scheerer 1st generation route, we used tethered aminohydroxylation 1st generation conditions on TA substrate **9**. We made our own batch of *t*-butyl hypochlorite to use for TA. Our first attempt of TA resulted in no reaction, but our second attempt produced multiple products. One product that seemed likely to be the desired product was proven incorrect with mass spectrometry. Since *t*-butyl hypochlorite has a short shelf life and we were concerned that its degradation was the reason for our problems, we performed TA on a known model substrate, which yielded no reaction. We made a new batch of *t*-butyl hypochlorite, which we tested on our model substrate and desired product appeared. We tried TA on the homoallylic carbamate again and the reaction generated many products. The ^{1}H NMR spectra of these products did not resemble what the desired product should look like. Next we bought *t*-butyl hypochlorite, which we used on the model substrate. Desired product was afforded, so we tried TA again with substrate **9**. However, the reaction gave many products and what may have desired product was disproved with mass spectrometry. There is a possibility that 10-15% desired product was generated since starting material was completely consumed, but with many byproducts it was difficult to tell. In addition possible chlorination of the alkene may have occurred and diastereomers of the desired product. Therefore, after many valid attempts we decided we should consider TA 3rd generation conditions.

However, using 3rd generation conditions meant rewriting the synthetic route (**Scheme 2.12**). The desired TA substrate was prepared starting with cyclic lactone **7**.

Scheme 2.12: Synthetic route toward TA using 3rd generation protocol
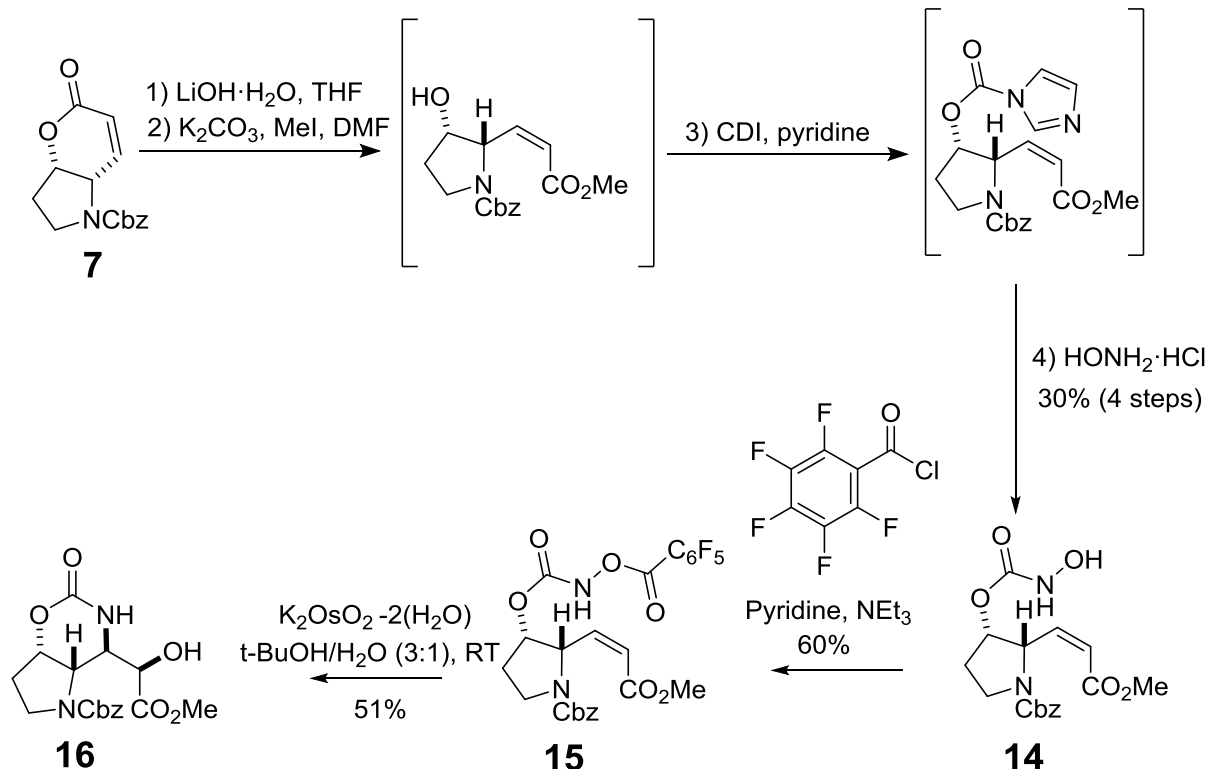
Opening of cyclic lactone **7** to the unsaturated ester was accomplished with saponification using lithium hydroxide. A subsequent esterification with MeI was performed on the intermediate carboxylic acid. Instead of using trichloroacetyl isocyanate, we used carbonyldiimidazole (CDI) to functionalize the nitrogen, in order to create hydroxylamine carbamate **14**. Over four steps **14** was afforded in 30% and the carboxylic acid intermediate was generated in 20% yield. Activated hydroxylamine carbamate **14** allowed us to perform an acylation with 2,3,4,5,6-pentafluorobenzoyl chloride. With installation of the reoxidant we could proceed to using TA 3rd generation conditions on aroyloxycarbamate **15**. Cyclic carbamate **16** was formed with 51% yield and a single diastereomer was formed. TA provides high stereoselectivity due to 1,3-allylic strain minimization. A(1,3) strain results from the interaction between substituents on the ends of an alkene. This strain energy is minimized by the largest substituent being in plane with

hydrogen. Preferred conformation of substrate **9** includes the allylic alcohol substituent and Cbz group in plane with the hydrogen (**Scheme 2.13**). The preferred conformation of **15** is predicted to be the same as **9** except with functional group differences. The tethered nitrogen has free rotation, but is still restricted; therefore, regioselectivity is controlled. Minimized A(1,3) strain of the *Z*-olefin reinforces the osmium species to preferentially attack from the top face and results in an intramolecular reaction; thus, addition results in the tethered nitrogen and the resulting alcohol *syn* to the hydrogen.

Scheme 2.13: Conformational analysis of TA 1st and 3rd generation substrates
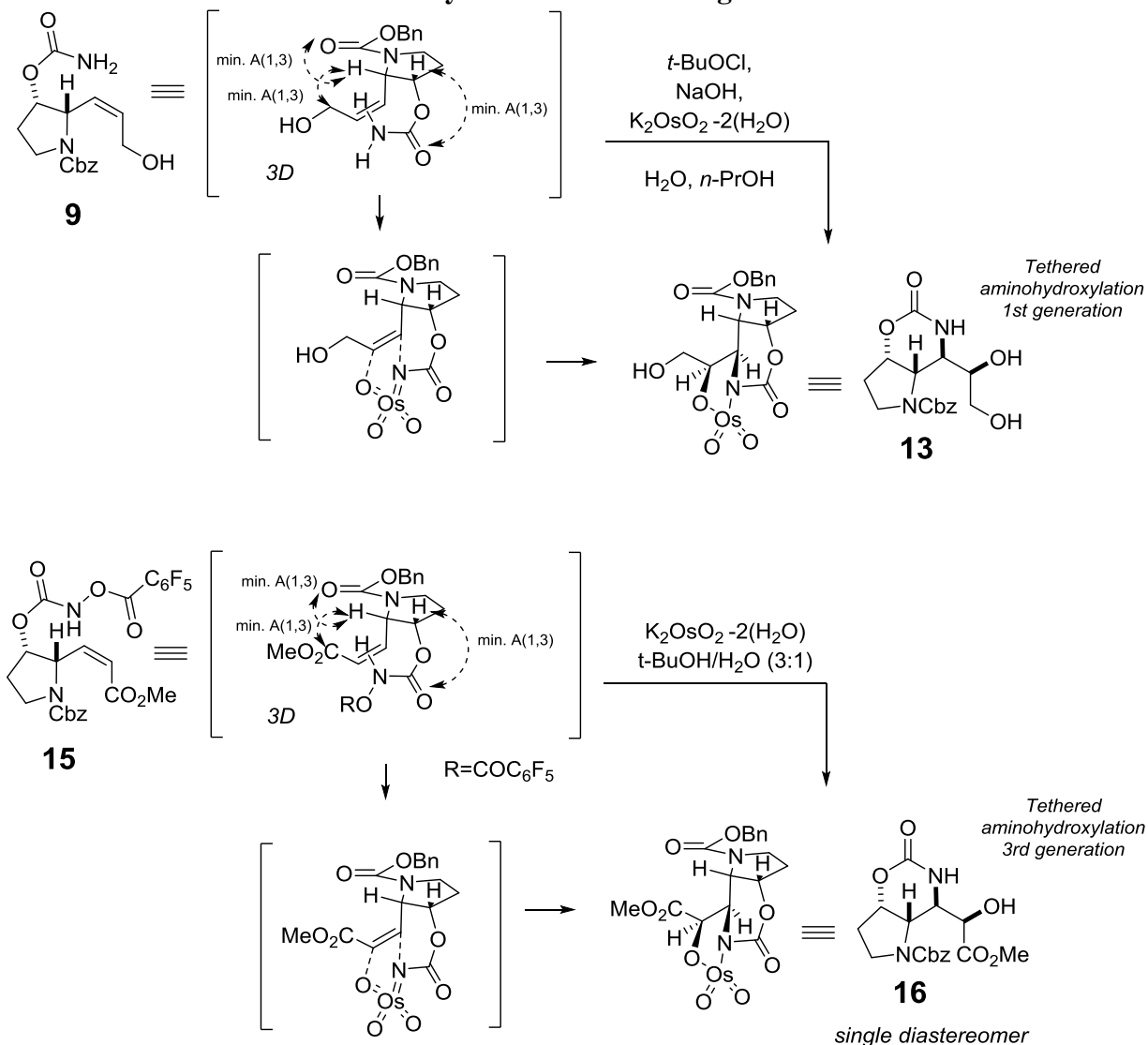
Scheme 2.14: Proposed synthetic route toward (+)-loline skeleton
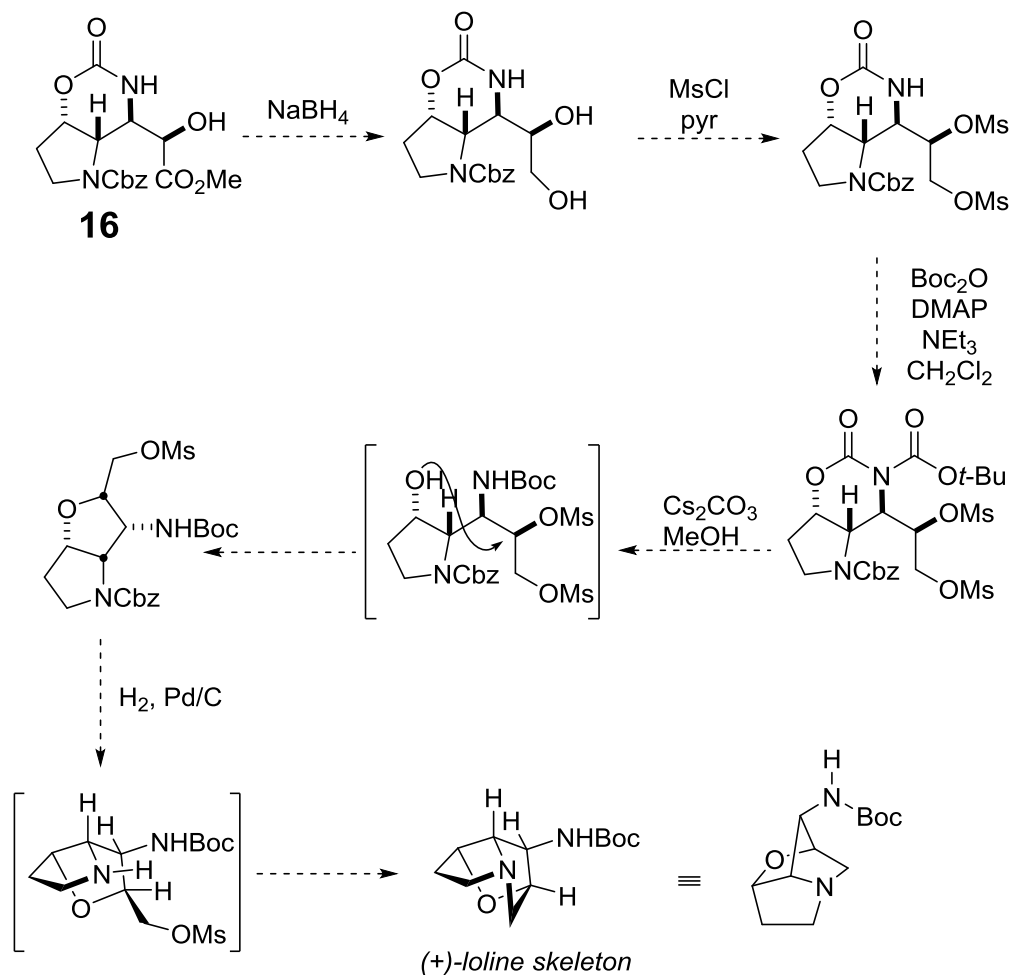
(+)-loline skeleton

With the four contiguous stereocenters in place, the rest of the synthesis has yet to be completed. The proposed route toward (+)-loline skeleton requires installation of the strained ether bridge. Starting with cyclic carbamate **16**, bis-mesylation occurs with methanesulfonyl chloride and di-*tert*-butyl dicarbonate should yield an imide (**Scheme 2.14**). The protected imide should allow for regioselective cleavage of the endocyclic carbamate and then the Cbz moiety is cleaved using hydrogen with palladium to generate the tricyclic Boc-norloline. From this point more than one loline alkaloid may be generated. For example, TFA could be used to cleave Boc functional group and then acetic anhydride should afford (+)-acetylnorloline, which is a total of 18 steps to this point.

Discussion:

The synthetic route discussed contains key advantages over Scheerer 1st generation synthesis. First, the Scheerer 2nd generation synthesis generates asymmetric loline compared to formation of racemic loline in the first generation route (**Table 2.3**). Second, fewer steps are employed toward TA substrate; only 11 steps instead of 12 steps. Third, the change in the nitrogen protecting group allows for better regioselectivity during the course of the synthesis. Most importantly the stereoselectivity and regioselectivity employed in this route will prove useful for the needed loline standard for biological testing, which the first generation could not adequately provide.

Table 2.3: Comparison of Scheerer loline syntheses

	Scheerer Syntheses of loline	
	1st	*2nd*
Year	2011	Current
Steps	19	18 (to (+)-acetylnorloline)
Stereoisomerism	racemic	asymmetric
Starting Material	N-Boc-2-azetidinone	(S)-4-amino-2-hydroxybutanoic acid
Nitrogen PG	Boc	Cbz
TA Protocol	1st	3rd

Highlights of this synthetic route include optimization of ring closing metathesis to yield close to 100%. In addition, although we had precedent from the first generation, the unexpected hindrances we faced during α, β-unsaturated ester reduction and the tethered aminohydroxylation must be due to the change in the nitrogen protecting group from Boc to Cbz. The addition of a Cbz moiety may be causing steric issues that cause an undesirable conformation not favorable

for TA stereoselectivity. As a result, chlorination of the alkene may be a more competitive reaction. After many trials with hydride reductants, simply adding a Lewis acid in combination with DIBAL-H helps the stable tetrahedral intermediate formed at -78 °C collapse, therefore allowing the reduction of the aldehyde to occur faster than the hydride transfer to the ester. Without the Lewis acid, elimination of the aldehyde is slower than the hydride transfer possibly due to reinforced stabilization of the tetrahedral intermediate from Cbz moiety. Furthermore, once we utilized TA 3rd generation protocol the desired product was formed with no byproducts and as a single diastereomer. A(1,3) strain reinforced the correct conformation of the cyclic carbamate and allowed us to proceed to the loline skeleton. With all stereocenters intact simple transformations should afford asymmetric loline. Future endeavors will investigate ways to shorten the route. Currently, Hoveyda is using one of his experimental catalysts on diol **4**, which could potentially bypass acylation and RCM to afford cyclic lactone **7**.

Conclusion:

Stereoselective synthesis installing the carbon framework of the loline skeleton has been achieved using Scheerer 2nd generation. Synthesis after the tethered aminohydroxylation remains to be completed, but the subsequent steps follow strong precedent from Scheerer 1st generation, so there is little concern that the rest of the synthesis will go according to plan. Since generation of cyclic carbamate **16** has been performed only twice, optimization of TA 3rd generation protocol should occur, especially since experiments by Donohoe claim such high yields using these conditions. Larger scale and diagnosis of other products formed during the course of the reaction should lead to higher yields. In addition, since our synthesis includes formation of a general loline core, multiple loline alkaloids can be synthesized, which only Trauner and coworkers have achieved. Our route is competitive because we provide an asymmetric route to multiple loline alkaloids, which allows for greater quantities of loline standards to be used for biological testing (**Table 2.4**). In addition, our route can branch off at methyl ester carbamate **8** and lead to isotopically labeled putative biosynthetic precursors, which will be used for feeding tests.

Table 2.4: Comparison of Scheerer 2nd generation synthesis to past loline syntheses

| Author	Year	Steps	Total Yield	Stereoisomerism
Tufariello	1986	12	24%	racemic
White	2001	22	2.1%	asymmetric
Scheerer 1st	2011	19	2.5%	racemic
Trauner	2011	10	35%	asymmetric
Scheerer 2nd	current	18	n.d.	asymmetric

References:

1. Li, G.; Chang, H. T.; Sharpless, K. B. *Angew. Chem. Int. Ed. in English* **1996**, *35*, 451-454.
2. Donohoe, T. J.; Callens, C. K. a; Flores, A.; Lacy, A. R.; Rathi, A. H. *Chem. Eur. J.* **2011**, 17, 58-76.
3. Donohoe, T. J.; Johnson, P. D.; Cowley, A.; Keenan, M. *J. Am. Chem. Soc.* **2002**, *124*, 12934-12935.
4. Donohoe, T. J.; Callens, C. K.; Lacy, A. R.; Winter, C. *Eur. J. Org. Chem.* **2012**, *2012*, 655-663.
5. Donohoe, T. J.; Chughtai, M. J.; Klauber, D. J.; Griffin, D.; Campbell, A. D. *J. Am. Chem. Soc.* **2006**, *128*, 2514-2515.
6. Donohoe, T. J.; Bataille, C. J.; Gattrell, W.; Kloesges, J.; Rossignol, E. *Org. Lett.* **2007**, *9*, 1725-1728.
7. Batey, R. A.; MacKay, D. B.; Santhakumar, V. *J. Am. Chem. Soc.* **1999**, *121*, 5075-5076.
8. Grubbs, R. H.; Miller, S. J.; Fu, G. C. *Acc. Chem. Res.* **1995**, *28*, 446-452.
9. Schrodi, Y.; Pederson, R. L. *Aldrichimica Acta* **2007**, *40*, 45-52.
10. Batey, R. A.; Mackay, D. B.; Santhakumar, V. *J. Am. Chem. Soc.* **1999**, *121,* 5075-5076.
11. Campeau, L. C.; Stuart, D. R.; Fagnou, K. *Aldrichimica Acta* **2007**, *40*, 35-41.
12. Luche, J.-L.; Gemal, A.L. *J.Chem. Soc.* **1978**, 976-977.
13. Encyclopedia of reagents for organic synthesis 2nd edition, book 8, Wiley, editors: Leo A. Paquette, David Crich, Philip L. Fuchs, Gary A. Molander; 2009
14. Brown, H. C.; Narasimhan, S.; Choi, Y. M., J. *J. Org. Chem.*, **1982**, *47*, 4702-4708.
15. Batey, R. A.; Mackay, D. B.; Santhakumar, V. *Tetrahedron* **1999**, 5075-5076.
16. Petasis, N. A.; Akritopoulou, I. *Tetrahedron Lett*. **1993**, *34*, 583-586.

EXPERIMENTAL PROCEDURES:

General Information. All reactions were carried out under an atmosphere of nitrogen in flame or oven-dried glassware with magnetic stirring unless otherwise indicated. Dichloromethane was distilled from CaH_2 prior to use. All reagents were used as received unless otherwise noted. Flash column chromatography was performed using SiliCycle siliaflash P60 silica gel (230–400 mesh). Analytical thin layer chromatography was performed on SiliCycle 60Å glass plates. Visualization was accomplished with UV light, anisaldehyde, ceric ammonium molybdate, potassium permanganate, or ninhydrin followed by heating. Film infrared spectra were recorded using a Digilab FTS 7000 FTIR spectrophotometer. Single crystal determinations were carried out using a Bruker *SMART Apex II* diffractometer using graphite-monochromated Cu Kα radiation. ^{1}H NMR spectra were recorded on a Varian Mercury 400 (400 MHz) spectrometer are reported in ppm using solvent as an internal standard ($CDCl_3$ at 7.26 ppm) or tetramethylsilane (0.00 ppm). The NMR spectra of all compounds containing carboxybenzyl (Cbz) residues are complicated by carbamate rotamers. Proton-decoupled ^{13}C-NMR spectra were recorded on a Mercury 400 (100 MHz) spectrometer and are reported in ppm using solvent as an internal standard ($CDCl_3$ at 77.00 ppm). ^{13}C-NMR employing the APT sequence were solved in which methylene and quaternary carbons = even (e) and methyl and methine carbons = odd (o). All compounds were judged to be homogeneous (>95% purity) by 1H and 13C NMR spectroscopy. Mass spectra data analysis was obtained through positive electrospray ionization (w/ NaCl) on a Bruker 12 Tesla APEX–Qe FTICR-MS with and Apollo II ion source.

1   **2**
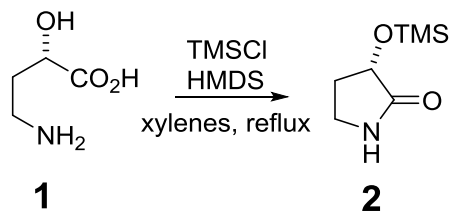
Preparation of (*S*)-3-((trimethylsilyl)oxy)pyrrolidin-2-one (2): Chlorotrimethylsilane

(0.270 mL, 2.1 mmol, 0.05 equiv) was added to a stirred mixture of (S)-4-amino-2-

hydroxybutanoic acid **1** (42.0 mmol), xylene (100 mL), and hexamethyldisilazane

(61.5 mL, 294 mmol, 7.0 equiv) at room temperature. The reaction mixture was heated

to reflux for 12 h, cooled to room temperature and diluted with absolute ethanol (200

mL). The solvents were removed under reduced pressure, and the crude product was

purified by flash chromatography on silica gel (elution: 20→100% EtOAc in

hexanes) to yield the light brown solid **2** (6.468 g, 89% yield): TLC (60% EtOAc in hexanes),

R*f*: 0.25 (UV, CAM); Spectral data for **2** matches published data.[14]

2   **3**
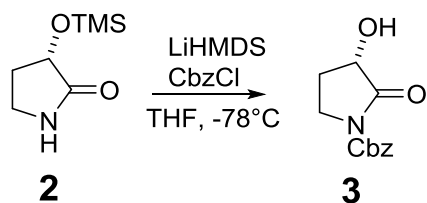
Synthesis of (*S*)-benzyl 3-hydroxy-2-oxopyrrolidine-1-carboxylate (3): To a solution

of **2** (0.112 g, 0.67 mmol) in THF (5 mL) at −78 °C was added LiHMDS (soln in

THF, 0.63 mmol, 0.95 equiv) dropwise over 5 min. After stirring 0.5 h at −78 °C, CbzCl

(0.120 g, 0.70 mmol, 1.05 equiv) was added to the reaction dropwise. The solution was

warmed to 23 °C over 1 h and quenched with aqueous hydrogen chloride (10

mL). The reaction mixture was then poured into a separatory funnel, diluted with ethyl

acetate (10 mL), and the organic layer removed. The aqueous layer was extracted with

additional ethyl acetate (2 x 12 mL). The organic layers were combined and washed

with brine (2 x 10 mL), dried (Na$_2$SO$_4$), and concentrated *in vacuo*. The resulting white

powder was purified by flash column chromatography on silica gel to afford **3** (0.104 g,

66% yield) as a white powder: mp 99.8–100.7 °C: TLC (60% EtOAc in hexanes), R*f*:

0.70 (UV, CAM); [α]D^{25} = – 63.9 (c = 1.94, CH$_2$Cl$_2$); IR (film) 3448, 3085, 3028, 2989,

2879, 1778, 1689, 1385, 1282, 1227 cm^{-1}; The spectra of **3** were complicated by imide

rotamers. ^{1}H NMR (400 MHz, CDCl$_3$) δ 7.40 (m, 5H, ArH), 5.29 (s, 2H, PhCH$_2$OR), 4.38

(m, 1H), 3.89 (m, 1H, C5aH), 3.60– 3.53 (td, J$_1$ = 6.6 Hz, J$_2$ = 10.5 Hz, 1H, C5bH),

2.48–2.42 (m, 1H, C6aH), 2.00–1.94 (m, 1H, C6bH); ^{13}C NMR (100 MHz, CDCl$_3$) δ

174.4, 151.1, 134.9, 128.6, 128.5, 128.2, 77.2, 70.4, 68.3, 42.1, 27.0; HRMS (ES+):

Exact mass calcd for C$_{12}$H$_{13}$NO$_4$Na^{+}[M+Na]$^{+}$, 258.0737. Found 258.0734.
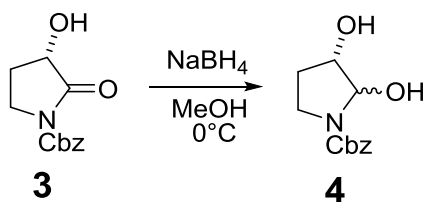
Synthesis of benzyl (3*S*)-2,3-dihydroxypyrrolidine-1-carboxylate (4): To a solution of

compound **3** (0.020 g, 0.085 mmol) in MeOH (0.70 mL) at 0 oC was added sodium borohydride

(0.006 g, 0.043 mmol, 0.5 equiv) in one portion. After stirring 0.5 h at 0 °C, the reaction was

quenched with sat. ammonium chloride (2 mL). The organic layer was removed and the

aqueous layer extracted with ether (3 x 5 mL). The organic fractions were combined,

dried (Na$_2$SO$_4$), and concentrated *in vacuo*. The resulting white powder **4** (0.020, 0.084

mmol, 99% yield) was used without further purification: TLC (60% EtOAc in hexanes), R*f*:

0.40 (UV, CAM); Spectral data for **4** matches published data.[15]
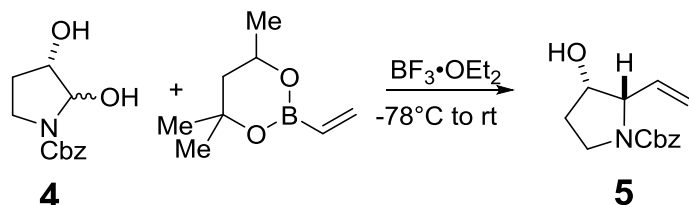
Synthesis of benzyl (3*S*)-3-hydroxy-2-vinylpyrrolidine-1-carboxylate (5): To a solution of the diol **4** (675 mg, 2.85 mmol) and boronate (482 mg, 3.13 mmol, 1.1 equiv) in DCM (20 mL) at −78 °C was added dropwise BF$_3$-EtO$_2$ (1.40 mL, 11.4 mmol, 4 equiv). The solution was warmed to 0 °C for 2 h and stirred at room temperature for an additional 3.5 h. The reaction was quenched with sat. NaHCO$_3$ (10 mL) and the mixture was transferred to a separatory funnel. The organic layer was removed and the aqueous layer was extracted with chloroform (5 x 5 mL). The organic fractions were combined and washed with brine (50 mL), dried (Na$_2$SO$_4$), and concentrated *in vacuo*. The resulting yellow oil was purified by flash column chromatography on silica gel (elution: 20→80 EtOAc in hexanes) to afford **5** (506 mg, 72% yield) as a clear oil: TLC (60% EtOAc in hexanes), R*f*. 0.40 (UV, CAM); $[\alpha]_D^{25}$ = −1.09 (c = 0.93, DCM); IR (film) 3419, 3083, 3072, 3033, 2978, 2951, 2894, 2361, 1956, 1698, 1592, 1540, 1480, 1448, 1357, 1257, 1213 cm^{-1}; The spectra of **5** were complicated by amide rotamers. ^{1}H NMR (400 MHz, CDCl$_3$) 7.33 (m, 5H, ArH), 5.81 (m, 1H), 5.22 (m, 2H), 5.09 (m, 2H), 4.35 (m, 2H), 3.56 (m, 2H), 2.23 (1H), 2.06 (m, 1H), 1.88 (m, 1H); ^{13}C (100 MHz, CDCl$_3$) δ 136.6, 133.9, 133.5, 128.4, 128.3, 127.8, 118.2, 117.9, 72.3, 71.8, 66.7, 62.9, 62.3, 43.7, 31.6 30.8; HRMS (ES+): Exact mass calcd for C$_{14}$H$_{17}$NO$_3$Na$^+$ [M+Na]$^+$, 270.1100. Found 270.1099.
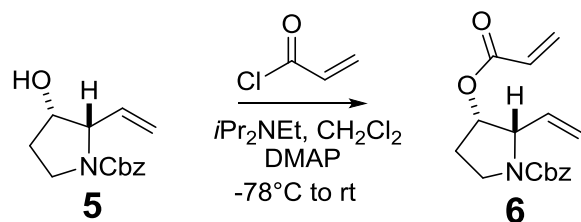
Synthesis of (2R,3S)-benzyl 3-(acryloyloxy)-2-vinylpyrrolidine-1-carboxylate (6): Compound

5 (357.1 mg, 1.45 mmol) was added to a flame dried flask and placed under N_2. The oil was

dissolved in CH_2Cl_2 (6 mL) and iPr$_2$NEt (1.26 mL, 7.23 mmol) and DMAP (12 mg, 0.072 mmol)

were added and cooled to −78 °C. In a separate flame dried pear flask under N_2, acryloyl

chloride (0.36 mL, 4.35 mmol) was diluted with CH_2Cl_2 (3 mL). The acryloyl chloride solution

was added dropwise over 7 minutes via Teflon cannula. After stirring 1 h at −78 °C, the reaction

was warmed to rt for 0.5 h and then quenched with saturated ammonium chloride (3 mL). The

organic layer was removed and the aqueous layer extracted with CH_2Cl_2 (4 x 4 mL). The

organic fractions were combined, washed with $NaHCO_3$ (4 mL), dried (Na_2SO_4), filtered, and

concentrated *in vacuo*. The resulting residue was purified by flash chromatography on silica gel

(elution: 10%→45% EtOAc in hexane) to afford **6** (319 mg, 75% yield) as a pale yellow oil:

TLC (40% EtOAc in Hexanes), Rf: 0.50 (UV, CAM); $[\alpha]_D^{25}$ = −37.9 (c = 1.19, CH_2Cl_2); IR

(film) 3066, 3033, 2985, 2955, 2892, 2361, 2339, 1723, 1703, 1635, 1406, 1355, 1296, 1267,

1190, 1129, 1106, 1069, 1052 cm^{-1}; The spectra of **6** were complicated by of amide rotamers.

^{1}H NMR (400 MHz, CDCl$_3$) δ 7.32 (m, 5H, ArH), 6.42-6.38 (d, J = 17.2, 1H), 6.13–6.06 (dd, J_1

= 17.2 Hz, J_2 = 10.2 Hz, 1H), 5.85-5.82 (d, J = 10.2 Hz, 1H), 5.68 (br. s., 1H), 5.25-5.08 (m,

5H), 4.67-4.63 (t, J = 6.6 Hz, 1H), 3.58-3.47 (m, 2H), 2.24-2.17 & 2.07-1.98 (m, 2H); ^{13}C NMR

(100 MHz, CDCl$_3$) δ 165.1, 136.5, 132.5, 131.4, 127.9, 117.4, 73.4, 66.8, 60.6, 43.1, 28.2;

HRMS (ES+): Exact mass calcd for C$_{17}$H$_{19}$NO$_4$Na$^+$ [M+Na]$^+$, 324.1206. Found 324.1204.
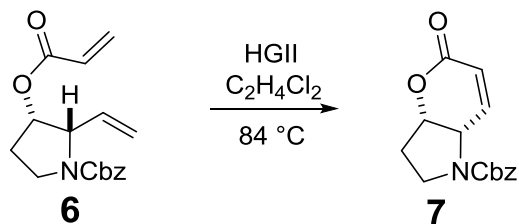
Synthesis of benzyl (3a*S*,7a*S*)-5-oxo-3,3a,5,7a-tetrahydropyrano[3,2-b]pyrrole-1(2H)-carboxylate (7): Compound **6** (294 mg, 0.98 mmol) was added to a flame dried two-neck flask and placed under N_2. Dichloroethane (19.7 mL) was added and the reaction mixture was heated to 84 °C for 10 minutes. Hoveyda-Grubbs Second Generation catalyst was added (45.7, 0.068 mmol). After stirring at reflux (84 °C) for 15 h under N_2, the reaction mixture was cooled to room temperature and concentrated *in vacuo*. The resulting residue was purified by flash chromatography on silica gel (elution: 15%→70% EtOAc in hexane) to afford **7** (242 mg, 90% yield) as a dark brown oil: TLC (60% EtOAc in Hexanes), R*f*: 0.40 (UV, CAM); $[\alpha]_D^{25} = +228$ (c = 0.19, CH_2Cl_2); IR (film) 3063, 2955, 2892, 2361, 2339, 1729, 1700, 1555, 1418, 1358, 1333, 1249, 1207, 1109, 1047 cm^{-1}; The spectra of **7** were complicated by amide rotamers. ^1H NMR (400 MHz, $CDCl_3$) δ 7.36 (m, 5H, ArH), 7.23–7.19 & 6.91-6.87 (dd, $J_1 = 10.2$ Hz, $J_2 = 4.8$ Hz, 1H), 6.07–6.01 (t, $J = 10.2$ Hz, 1H), 5.21–5.06 (m, 3H), 4.32 (s, 1H), 3.72-3.67 & 3.63-3.56 (m, 2H), 2.28-2.18 (m, 2H); ^{13}C NMR (100 MHz, $CDCl_3$) δ 161.8, 154.5, 142.3, 136.1, 128.4, 127.9, 120.9, 79.2, 67.3, 51.3, 44.6, 31.2; HRMS (ES+): Exact mass calcd for $C_{15}H_{15}NO_4Na^+$ [M+Na]$^+$, 296.0893. Found 296.0894.
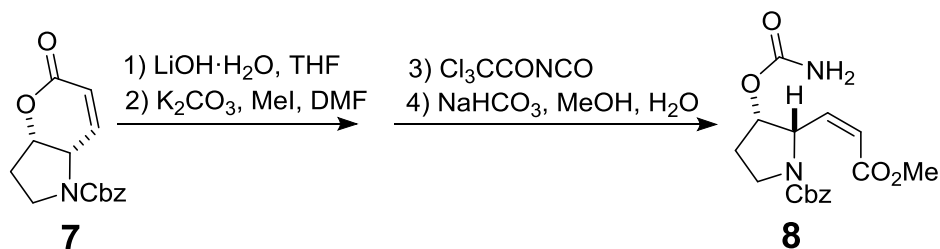
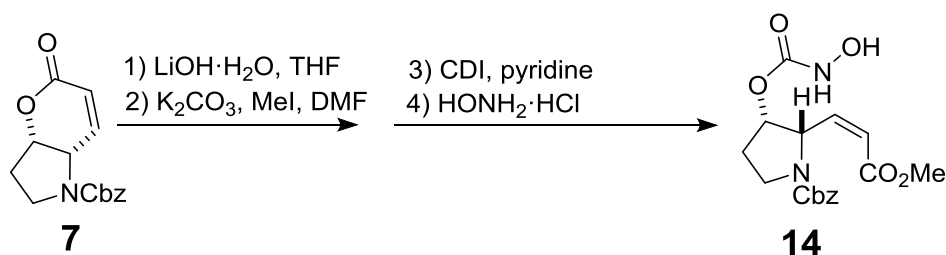**Synthesis of benzyl (2*S*,3*S*)-3-(carbamoyloxy)-2-((*Z*)-3-methoxy-3-oxoprop-1-en-1-yl)pyrrolidine-1-carboxylate (8)**: To a solution of **7** (283 mg, 1.03 mmol) in THF (5.3 mL) and H$_2$O (1.7 mL) was added LiOH• H$_2$O (54 mg, 1.29 mmol, 1.25 equiv) at ambient temperature. After stirring for 1 h, the reaction mixture was transferred to a separatory funnel and partitioned between 0.2 M HCl (10 mL) and EtOAc (5 mL). The organic layer was removed, and the aqueous layer was extracted with additional EtOAc (5 x 5 mL). The organic fractions were combined and washed with brine (40 mL), dried (Na$_2$SO$_4$), and concentrated *in vacuo*. The resulting dark oil was dissolved in DMF (5 mL) at 23 °C and K$_2$CO$_3$ (171 mg, 1.24 mmol, 1.2 equiv) and MeI (0.642 mL, 10.3 mmol, 10.0 equiv) were added. After stirring for 2 h, the reaction mixture was transferred to a separatory funnel and diluted with a brine and 1.0 M HCl solution (10 mL, 10:1 brine:HCl) and extracted with CHCl$_3$ (5 mL). The organic layer was removed, and the aqueous layer was extracted with CHCl$_3$ (5 x 5 mL). The organic layers were combined, washed with brine (40 mL), dried (Na$_2$SO$_4$), and concentrated *in vacuo*. The resulting dark oil was dissolved in CH$_2$Cl$_2$ (5 mL) and cooled to 0 °C. Trichloroacetyl isocyanate (0.182 mL, 1.55 mmol. 1.5 equiv) was added and the reaction was stirred for 30 min and concentrated *in vacuo*. The residue was dissolved in MeOH (4.0 mL) and H$_2$O (1.0 mL) and cooled to 0 °C. To this solution was added NaHCO$_3$ (173 mg, 2.06 mmol, 2 equiv) and the reaction was allowed to warm to ambient temperature overnight. The reaction mixture was transferred to a separatory funnel and partitioned between brine (5 mL) and CHCl$_3$ (5 mL) and the organic layer was removed. The aqueous layer was extracted with CHCl$_3$ (5 x 5 mL) and the organic layers were

combined, washed with brine (40 mL), dried (Na$_2$SO$_4$), and concentrated *in vacuo*. The resulting

dark oil was purified by flash column chromatography (elution: 40%→80% EtOAc in hexanes)

to afford **8** (243 mg, 70% yield over 3 steps) as a white solid: TLC (60% EtOAc in hexanes), R*f*:

0.30 (UV, CAM); [α]$_D^{25}$ = +81.9 (c = 1.67, CH$_2$Cl$_2$); IR (film): 3399, 2954, 2885, 1715, 1689,

1606, 1415, 1348, 1198, 1172, 1105, 1043 cm^{-1}; The spectra of **8** were complicated by amide

rotamers. ^{1}H NMR (400 MHz, CDCl$_3$) δ 7.33 (m, 5H, ArH), 6.17 (m, 1H, 5.87 (m, 1H, *J* = 10.9

Hz), 5.54 (s, 2H), 5.10 (m, 4H), 3.67 (m, 4H), 3.56 (m, 1 H), 2.09 (m, 2H); ^{13}C NMR (100 MHz,

CDCl$_3$) δ 165.93, 155.69, 154.88, 146.43, 136.37, 128.18, 127.89, 127.73, 127.58, 120.18, 77.32,

76.18, 75.70, 66.84, 59.45, 58.36, 51.25, 51.23, 44.99, 44.69, 31.17, 30.59 HRMS (ES+): Exact

mass calcd for C$_{17}$H$_{20}$N$_2$O$_6$Na$^+$ [M+Na]$^+$, 371.1214. Found 371.1215.
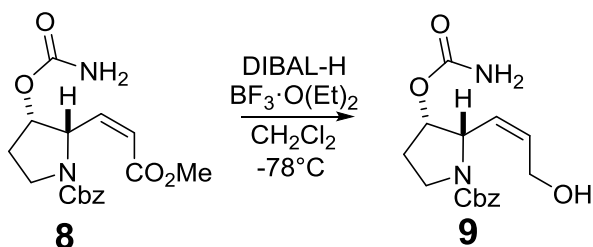
Synthesis of benzyl (2*S*,3*S*)-3-(carbamoyloxy)-2-((*Z*)-3-hydroxyprop-1-en-1-yl)pyrrolidine-1-carboxylate (9): Compound **8** (187 mg, 0.54 mmol) was dissolved in CH$_2$Cl$_2$ (7.2 mL) and

cooled to −78 °C while stirring under N$_2$. BF$_3$·OEt$_2$ (0.23 mL) was added slowly and stirred for

5 min. A solution of DIBAL-H (0.5 M in CH$_2$Cl$_2$, 4.32 mL, 2.16 mmol) was added dropwise for

10 min. After 0.5 h the reaction was quenched with EtOAc (1 mL) and stirred for 5 min. The

reaction was warmed to rt and concentrated HCl (5 mL) was added and stirred for 5 min. EtOAc

(10 mL) was added and the reaction mixed was transferred to a separatory funnel. The aqueous

layer was extracted with EtOAc (3 x 10 mL) and the combined organic layers were washed with

NaHCO$_3$ (10 mL). The removed organic layers were dried (Na2SO4), filtered, and concentrated

in vacuo. The resulting residue was purified by flash chromatography on silica gel (elution: 55% →100% EtOAc in hexane) to afford **9** (95.7 mg, 56% yield) as a white solid: TLC (80% EtOAc in Hexanes), R*f*: 0.25 (UV, CAM); $[\alpha]_D^{25}$ = –42.2 (c = 1.06, CH_2Cl_2); IR (film) 3816, 3406, 3213, 2953, 1696, 1421, 1344, 1207, 1086 cm^{-1}; The spectra of **9** were complicated by amide rotamers. ^{1}H NMR (400 MHz, $CDCl_3$) δ 7.34 (m, 5H, ArH), 5.96 (m, 1H), 5.74 (m, 1H), 5.43–5.29 (m, 1H), 5.12-5.05 (m, 4H), 4.34 (m, 1H), 4.05 & 3.74 (m, 2H), 2.37 (br. s., OH), 2.19-2.16 & 2.06-2.04 (m, 2H); ^{13}C NMR (100 MHz, $CDCl_3$) δ 156.2, 154.6, 136.2, 132.7, 128.8, 128.5, 127.8, 127.5, 125.7, 74.2, 73.2, 67.1, 55.3, 43.3, 29.2; HRMS (ES+): Exact mass calcd for $C_{16}H_{20}N_2O_5Na^+$ [M+Na]$^+$, 343.1264 Found 343.1266.


Synthesis of benzyl (2*S*,3*S*)-3-((hydroxycarbamoyl)oxy)-2-((*Z*)-3-methoxy-3-oxoprop-1-en-1-yl)pyrrolidine-1-carboxylate (14): The resulting residue was purified by flash chromatography on silica gel (elution: 30%→100% EtOAc in hexane): TLC (60% EtOAC in Hexanes), R*f:* 0.20 (UV, CAM); $[\alpha]_D^{25}$ = +71.3 (c = 1.03, CH_2Cl_2); IR(film) 3303, 3066, 3032, 2993, 2954, 2898, 1714, 1617, 1539, 1455, 1357, 1255, 1199, 1110, 1034, 996, 918, 816, 765, 733, 699, 667 cm^{-1}; The spectra of **14** were complicated by amide rotamers. ^{1}H NMR (400 MHz, $CDCl_3$) δ 7.75-7.71 (d, *J* = 18.8 Hz, 1H, NH), 7.55(br.s, 1H, OH), 7.34 (m, 5H, ArH), 6.13-6.05 (m, 1H), 5.88-5.78 (d, *J* = 10.4 Hz, 1H), 5.58-5.52 (m,2H), 5.11-5.08 (m, 2H), 3.67-3.49 (m, 5H), 2.037 (m, 2H) ^{13}C NMR (100 MHz, $CDCl_3$) δ 166.3, 166.1, 157.7, 155.0, 146.1, 136.1, 135.9, 128.3, 128.2, 127.8, 127.6, 120.4, 67.0, 58.5, 58.5, 51.3, 45.0, 44.6, 31.0, 30.5.
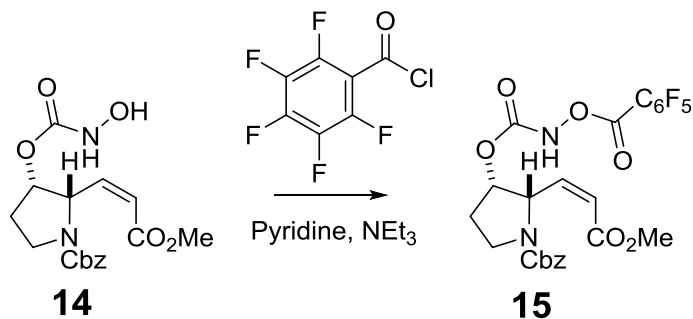
Synthesis of benzyl (2S,3S)-2-((Z)-3-methoxy-3-oxoprop-1-en-1-yl)-3-((((7,7,7,7,7-pentafluoro-7λ⁸-hepta-2,4,6-triynoyl)oxy)carbamoyl)oxy)pyrrolidine-1-carboxylate (15):

The resulting residue was purified by flash chromatography on silica gel (elution 20→70% EtOAc in hexanes): TLC (60% EtOAc in hexanes), R*f*: 0.60 (UV, CAM): $[\alpha]_D^{25}$ = +66.1 (c = 1.00, CHCl₃); IR(film) 3197,2953, 2903, 1923, 1866, 1789, 1760, 1701, 1653, 1576, 1503, 1416, 1359, 1326, 1255, 1184, 1105, 998, 912, 818, 755, 697 cm⁻¹; The spectra of **15** were complicated by amide rotamers. ¹H NMR (400 MHz, CDCl₃) δ 8.78 (br.s, 1H, NH), 7.50-7.18 (m, 5H, ArH), 6.15-6.03 (dd, 1H), 5.94-5.83 (dd, J = 10.9 Hz, 1H), 5.74 (s, 1H), 5.63-5.58 (d, 1H), 5.14-5.07 (m, 2H), 3.83-3.14 (m, 5H), 2.35-2.04 (m, 2H). ¹³C NMR (100 MHz, CDCl₃) δ 166.0, 158.2, 155.0, 154.7, 145.7, 128.5, 128.3, 128.0, 127.7, 120.9, 104.7, 78.3, 67.2, 58.8, 51.4, 45.2, 31.1, 30.7.
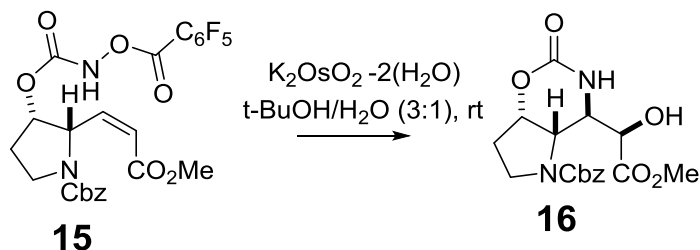
Synthesis of benzyl (4R,4aS,7aS)-4-((R)-1-hydroxy-2-methoxy-2-oxoethyl)-2-oxohexahydropyrrolo[2,3-e][1,3]oxazine-5(2H)-carboxylate (16): Compound **15** (97.7 mg, 0.18 mmol) was dissolved in *t*-BuOH/water solution (3:1, 20 mL/mmol). Solution of potassium

osmate dihydrate (4.5 mg, 6 mol%) in water (0.5 mL) was added dropwise over 10 min. After stirring at rt under N_2 for 1.5 h the reaction was quenched with addition of sodium sulfite (71 mg, 200 mg/mmol) and stirred for an additional 0.5 h. The solvent was azeotropically removed with toluene and chloroform and concentrated *in vacuo*. The resulting residue was purified by flash chromatography on silica gel (elution: 0%→10% MeOH in $CHCl_3$) to afford **16** (32.5 mg, 51% yield) as a clear oil: TLC (5% MeOH in Chloroform), R*f*: 0.33 (UV, CAM); $[\alpha]_D^{25} = +44$ (c = 1.63, $CHCl_3$); IR (film) 3326, 3017, 2954, 2907, 1744, 1696, 1536, 1414, 1355, 1212, 1112, 759 cm^{-1}; the spectra of **16** were complicated by amide rotamers. ^{1}H NMR (400 MHz, $CDCl_3$) δ 7.35 (m, 5H, ArH), 6.93 & 6.77 (m, 1H, NH), 5.13–5.06 (m, 3H), 4.77 (m, 1H), 4.47 & 4.29 (m, 2H), 4.02 (m, 1H), 3.83-3.72 (m, 3H), 3.53 & 3.48-3.41 (m, 2H), 2.20-2.16 & 1.99-1.96 (m, 2H); ^{13}C NMR (100 MHz, $CDCl_3$) δ 172.0, 155.5, 154.1, 136.0, 128.5, 128.2, 127.9, 79.2, 77.2, 72.8, 67.2, 53.8, 52.8, 44.7, 31.9.

400 Hz, CDCl₃

2

400 Hz, CDCl₃

2

400 Hz, CDCl₃

3

400 Hz, CDCl₃

3

400 Hz, CDCl₃

5

400 Hz, CDCl₃

5

400 Hz, CDCl₃

6

400 Hz, CDCl₃

6

400 Hz, CDCl₃

7

400 Hz, CDCl₃

7

400 Hz, CDCl₃

8

400 Hz, CDCl₃

8

400 Hz, CDCl₃

9

400 Hz, CDCl$_3$

9

400 Hz, CDCl₃

14

14

400 Hz, CDCl$_3$

400 Hz, CDCl₃

15

400 Hz, CDCl₃

15

400 Hz, CDCl₃

16

400 Hz, CDCl₃

16